Heat and spin transport in a cold atomic Fermi gas

Hyungwon Kim and David A. Huse
Physics Department, Princeton University, Princeton, New Jersey 08544, USA
(Received 12 September 2012; published 8 November 2012)

Motivated by recent experiments measuring the spin transport in ultracold unitary atomic Fermi gases [Sommer *et al.*, Nature (London) **472**, 201 (2011); Sommer *et al.*, New J. Phys. **13**, 055009 (2011)], we explore the theory of spin and heat transport in a three-dimensional spin-polarized atomic Fermi gas. We develop estimates of spin and thermal diffusivities and discuss magnetocaloric effects, namely the the spin Seebeck and spin Peltier effects. We estimate these transport coefficients using a Boltzmann kinetic equation in the classical regime and present experimentally accessible signatures of the spin Seebeck effect. We study an exactly solvable model that illustrates the role of momentum-dependent scattering in the magnetocaloric effects.

DOI: 10.1103/PhysRevA.86.053607 PACS number(s): 03.75.Ss, 51.10.+y, 05.20.Dd, 34.50.−s

I. INTRODUCTION

The transport properties of condensed-matter systems are often measured by driving currents externally and measuring the resulting voltages or temperature differences. In cold atomic gas clouds, on the other hand, transport is more often measured by setting up transient out-of-equilibrium initial conditions and measuring the subsequent relaxation towards equilibrium [1–6]. In the approximation that the cloud is isolated and has an infinite lifetime (no loss of atoms or exchange of energy with any degrees of freedom outside of the gas cloud), the conserved currents of interest include the energy current and currents of each of the atomic species present. In the absence of optical lattices or random potentials that violate momentum conservation, one can also ask about the transport of momentum (viscosity).

In this paper we consider the diffusive transport of heat and of atoms. We mostly focus on the case of a two-species Fermi gas with only interspecies contact interactions, but start with a somewhat more general discussion here. The system may, in addition to diffusive transport, also have underdamped or propagating sound or other "collective" modes. A gas cloud in a smooth trap will have such sound modes, with the longest-wavelength sound modes being the often-discussed collective modes of the cloud's oscillations within the trap. Here we consider a gas cloud in a smooth trap, with the cloud at global *mechanical* equilibrium, so that any pressure gradients in the cloud are sufficiently balanced by trapping forces that no underdamped sound or collective modes are excited. We also assume that the cloud is everywhere near *local* thermodynamic equilibrium, so the local temperature $T(\mathbf{r})$ and local chemical potentials $\mu_i(\mathbf{r})$ can be defined. However, the cloud may still have gradients in the local temperature and in the local chemical potentials of the various species of atoms. If the equilibrium equation of state of the system is known (for the unitary Fermi gas, see [7,8]), then measurements of the local densities of each species allows these gradients of T and the μ_i's to be measured. Thus, for example, the local densities can be used as local thermometers to allow a measurement of the thermal diffusivity by an approach similar to that used in [1,2] to measure the spin diffusivity (but with an initial temperature gradient instead of a composition gradient).

The transport currents that we examine in this paper are those that arise in linear response to these gradients. In a trap, convection currents may also appear in linear response, as temperature and/or composition gradients may produce density inhomogeneities, and the "heavier" regions of the gas cloud will sink towards the bottom of the trap while the "lighter" regions rise. These convection currents are damped by the viscosity. Convection will be strongest in wide clouds and should be much weaker in high-aspect-ratio clouds with the gradients in T and the μ_i's oriented along the long axis of the cloud. In most of this paper, for simplicity we consider a gas in a spatially uniform potential, so such convection currents do not appear in linear response. Then mechanical equilibrium is indeed a sufficient condition to have a convectionless gas [9].

Quite generally, a temperature gradient drives a heat current and a gradient of chemical potential difference drives a composition ("spin") current, consisting of opposing currents of the two (or more) atomic species. We call these "direct" responses to a temperature gradient and a gradient of chemical potential difference "primary currents." In addition to these "primary currents," there are the magnetocaloric currents, namely spin Seebeck currents (spin currents induced by a temperature gradient) and spin Peltier currents (heat currents induced by gradients of chemical potential difference). These magnetocaloric effects have been one of the central research topics in the field of spintronics [10]. The spin Seebeck effect [11,12] and the spin Peltier effect [13] have already been observed in condensed-matter systems, while they are yet to be detected in cold atomic clouds. In this paper we discuss the origin and the physics of these effects in a cold atomic Fermi gas and estimate how large these effects can be in realistic experiments.

Note that Ref. [14] discusses a rather different situation that they are also calling the "spin Seebeck effect": They consider an unpolarized gas with the two species at different temperatures (thus *not* in *local* equilibrium) and a gradient in this temperature difference. Also, Ref. [15] studies a different system, a "two terminal geometry," considering transport through a narrow constriction between two reservoirs held at different temperatures and chemical potentials. For this constriction, they discuss "off-diagonal" elements in the transport matrix which they call effective Seebeck and Peltier effects.

This paper begins with a general discussion of the two-species universal Fermi gas and an introduction of transport coefficients, spin and thermal diffusivities, spin Seebeck effect,

and spin Peltier effect. Then we present rough estimates of diffusivities and determine the signs of the spin Seebeck and spin Peltier effects based on physical arguments. In the following section, these qualitative descriptions are justified by approximate solutions of the Boltzmann transport equation in the classical regime. We then compute experimentally verifiable signals of the spin Seebeck effect. These results are tested against an exactly solvable model, namely atoms with a "Maxwellian" scattering cross section. We also use the Kubo formula to derive various general relations among the transport currents and coefficients.

The various effects discussed in this paper are probably most accessible experimentally for the unitary Fermi gas at temperatures of order of the Fermi temperature, where the diffusivities are at their smallest, so the diffusive relaxation towards equilibrium is slowest and most easily studied.

We set Boltzmann's constant $k_B = 1$ but explicitly keep Planck's constant $\hbar$.

II. UNIVERSAL FERMI GAS

The universal Fermi gas is a two-species Fermi gas with only contact (s-wave) inter-species interactions that is realized to a very good approximation in recent experiments with ultracold atoms [16,17]. We consider such a gas in three-dimensional space, with the two species having equal mass m. There is no optical lattice, only a possible smooth trap potential. The interaction is specified by the scattering length a, which can be set to any value in experiments by tuning through a Feshbach resonance [18,19]. For $a = 0$ this is the standard textbook noninteracting Fermi gas, while for weakly attractive a it is very close to the model used by Bardeen, Cooper, and Schrieffer (BCS) to explain superconductivity. Indeed, this system shows paired-fermion superfluidity at low temperatures. The limit of infinite $|a|$ is the strongly interacting unitary Fermi gas.

As is standard, we call the majority species with number density $n_\uparrow$ "up" and the minority species "down," $n_\downarrow \leqslant n_\uparrow$. The total number density, $n = n_\uparrow + n_\downarrow$, together with m and $\hbar$ set the characteristic length, time, and energy scales. The scaled dimensionless properties of this universal Fermi gas then depends on only three dimensionless parameters, which can be chosen to be $1/(k_F a)$, T/T_F, and the polarization $p = (n_\uparrow - n_\downarrow)/n$. We use a convention that the Fermi wave number and temperature, k_F and T_F, respectively, are defined by the total density, so that at high polarization $T_{F\downarrow} \ll T_F \approx T_{F\uparrow}$ and $k_{F\downarrow} \ll k_F \approx k_{F\uparrow}$. This universal Fermi gas has a variety of regimes of behavior: The polarization p can be low or zero so $n_\downarrow \cong n_\uparrow$ or it can be near one so $n_\downarrow \ll n_\uparrow$. The temperature can be higher, $T > T_{F\uparrow}$, or lower, $T < T_{F\downarrow}$, than both Fermi temperatures or, for $p > 0$, it can be in between them, $T_{F\downarrow} < T < T_{F\uparrow}$. The scattering can be near unitarity so $|k_F a|$ is of order one or more, or it can be far from unitarity so $|k_F a| \ll 1$. At high T it also matters whether $|a|$ is larger or smaller than the thermal de Broglie wavelength $\lambda \equiv \sqrt{2\pi\hbar^2/mT} \sim T^{-1/2}$. There are also important differences between the $a < 0$ (BCS side of the Feshbach resonance) and $a > 0$ (BEC side) regimes.

III. TRANSPORT

The conservation laws of this Fermi gas are total energy (E), total momentum ($\mathbf{\Pi}$), and the total number of each of the species ($N_\uparrow$ and $N_\downarrow$). The viscosity measures the transport of momentum, which we mostly do not consider here. Thus, we consider primarily the transport of atoms and of heat. If there is a nonuniform pressure in the system that is not balanced by a trapping potential, the gas will accelerate and this will produce free motion or propagating sound waves. Here we consider the diffusive spin and heat transport in a gas with no trapping potential and spatially uniform pressure P, so it is at mechanical equilibrium. The gas is near *local* thermodynamic equilibrium, but with possible weak gradients in the local temperature and/or the spin polarization. A smooth trap potential may be added via the local density approximation (LDA).

In general, an inhomogeneity of the Fermi gas consists of gradients in the local temperature and of the local densities of the two atomic species. Mechanical equilibrium imposes a constraint on these gradients and thus there are only two independent linear combinations of the three gradients. One way of describing the diffusive dynamics is in terms of the atomic densities n_i and the currents $\mathbf{j}_i$ of each species $i = \uparrow, \downarrow$, leaving the temperature and the heat current implicit, since they are dictated by the equilibrium equation of state, for example, $T(P, n_\uparrow, n_\downarrow)$. This description of the transport has the virtue that it is in terms of what appears to be the most accessible local observables in experiment, namely the local densities of each species. Since the system in the absence of a trapping potential is Galilean invariant, we have a certain amount of flexibility in what inertial frame we use to specify the currents. For most of this work, we consider the frame where the center of mass of the whole cloud is at rest and let the gas have long-wavelength temperature, density, and/or composition modulations, but always with a spatially uniform pressure. The diffusive currents are related to the density gradients as

$$\begin{pmatrix} \mathbf{j}_\uparrow \\ \mathbf{j}_\downarrow \end{pmatrix} = -\begin{pmatrix} \mathfrak{D}_{\uparrow\uparrow} & \mathfrak{D}_{\uparrow\downarrow} \\ \mathfrak{D}_{\downarrow\uparrow} & \mathfrak{D}_{\downarrow\downarrow} \end{pmatrix} \begin{pmatrix} \nabla n_\uparrow \\ \nabla n_\downarrow \end{pmatrix}. \tag{1}$$

The diffusion matrix in (1) has two eigenmodes. At zero polarization, the symmetry between $\uparrow$ and $\downarrow$ implies $\mathfrak{D}_{\uparrow\uparrow} = \mathfrak{D}_{\downarrow\downarrow}$ and $\mathfrak{D}_{\uparrow\downarrow} = \mathfrak{D}_{\downarrow\uparrow}$. Therefore, one eigenmode is odd under exchanging species, $\frac{1}{\sqrt{2}}(1, -1)$; the current in this odd mode carries only spin and no net density or energy. The other eigenmode is the even mode, $\frac{1}{\sqrt{2}}(1,1)$; the current in this even mode carries both net density and energy, but no spin. Away from zero polarization, when $n_\uparrow \neq n_\downarrow$, we no longer have this symmetry between species. The diffusive eigenmodes are then no longer purely spin or purely not spin; instead they are mixtures, thus producing the spin Seebeck and Peltier effects. The eigenmode where the currents of the two species are in opposite directions we call the "spin" mode with diffusivity $\mathfrak{D}_s$, while the other mode where they are parallel we call the "thermal" (or heat) mode with diffusivity $\mathfrak{D}_T$.

Another standard representation of the transport matrix in terms of the heat current $\mathbf{j}_{\text{heat}}$ and spin current $\mathbf{j}_{\text{spin}}$ is the

following:

$$\begin{pmatrix} \mathbf{j}_{\rm heat} \\ \mathbf{j}_{\rm spin} \end{pmatrix} = -\begin{pmatrix} \kappa & P_s \\ S_s & \sigma_s \end{pmatrix}\begin{pmatrix} \nabla T \\ \nabla(\mu_\uparrow - \mu_\downarrow) \end{pmatrix}, \tag{2}$$

where κ is the thermal conductivity and σ_s is the spin conductivity. S_s and P_s are the spin Seebeck and Peltier coefficients, respectively, and they are related by the Onsager relation, $P_s = TS_s$. This matrix explicitly shows the direct responses (diagonal elements) and magnetocaloric effects (off-diagonal elements) and is in the form that is given by the Kubo formula, as we discuss below.

The currents in (2) must be defined properly so that they are the transport currents, namely the currents of heat and spin relative to the average local motion of the gas. Let the local current density of atoms be $\mathbf{j}_n = \mathbf{j}_\uparrow + \mathbf{j}_\downarrow$. These atoms carry the average heat, sT, where s is the average entropy per particle, and the average spin polarization p. Therefore, the local heat and spin transport currents are

$$\mathbf{j}_{\rm heat} = \mathbf{j}_\epsilon - \mu_\uparrow \mathbf{j}_\uparrow - \mu_\downarrow \mathbf{j}_\downarrow - sT\mathbf{j}_n, \tag{3}$$

$$\begin{aligned} \mathbf{j}_{\rm spin} &= \frac{1}{2}\left(\mathbf{j}_\uparrow - \mathbf{j}_\downarrow - \frac{(n_\uparrow - n_\downarrow)}{n}\mathbf{j}_n\right) \\ &= \frac{n_\downarrow}{n}\mathbf{j}_\uparrow - \frac{n_\uparrow}{n}\mathbf{j}_\downarrow, \end{aligned} \tag{4}$$

where $\mathbf{j}_\epsilon$ is the local energy current. Since the above currents measure only the transport relative to the average motion of the gas, they are *reference frame independent*. For more details of definitions of currents (see, e.g., Ref [20]).

If the full equation of state of the system is known, then measurements of the pressure and the local densities can be converted to local temperatures and chemical potentials. However, the local density n and polarization p are directly observable without requiring knowledge of the equation of state, so yet another convenient form of the transport equations is

$$\begin{pmatrix} \mathbf{j}_{\rm heat} \\ \mathbf{j}_{\rm spin} \end{pmatrix} = -\begin{pmatrix} \kappa' & P_s' \\ S_s' & D_s \end{pmatrix}\begin{pmatrix} \nabla T \\ n\nabla p \end{pmatrix}. \tag{5}$$

At $p = 0$, we have $\kappa' = \kappa$ and $D_s = \mathfrak{D}_s$, but when $p \neq 0$ these quantities, in general, differ due to the mixing between spin and heat transport. It is possible that S_s' is the most directly accessible version of the spin Seebeck coefficient: If one can set up an initial condition at mechanical equilibrium and local thermodynamic equilibrium with a temperature gradient but no polarization gradient and then measure the resulting spin current, this is a measurement of S_s' and does not require knowledge of the equation of state.

Note that the three representations, Eqs. (1), (2), and (5), are related by the equation of state, the mechanical equilibrium condition, and definitions of spin and heat currents. Hence, they are *equivalent*.

IV. DIFFUSIVITIES

Let us first present rough "power-counting" estimates of the spin and thermal diffusivities, D_s and D_T, respectively. At the level of power counting the differences between the various possible definitions of these diffusivities are small and are ignored here. Previous work [1,21] on the unpolarized gas ($p = 0$) shows that D_s for $T > T_F$ is the larger of $\frac{\hbar}{m}(\frac{T}{T_F})^{3/2}$ and $\frac{\hbar}{mk_F^2a^2}\sqrt{\frac{T}{T_F}}$. In the recent experiment, which was performed at unitarity [1], this high-T behavior is observed, with significant deviations apparently beginning between $T = 2T_F$ and T_F as T_F is approached from above. Staying in this high-T regime, as we move to high polarization (p near 1) at a given n and T, the scattering time of species i is roughly $\tau_i \sim \frac{1}{n_j \sigma v_r}$, where $i \neq j$ and $v_r = |\mathbf{v}_\uparrow - \mathbf{v}_\downarrow|$ and σ is the s-wave scattering cross section [see Eq. (12)] evaluated at a typical value of momentum. Thus, the scattering time of the down atoms $\tau_\downarrow$ decreases by only a factor of two due to the increase of the density $n_\uparrow$ of the up atoms that they scatter from. The up atom scattering time $\tau_\uparrow$, on the other hand, increases by a factor of $n_\uparrow/n_\downarrow$ as the down atoms that they scatter from become dilute. At high polarization, the spin current consists of the down atoms moving with respect to the up atoms at typical speed $v_\downarrow \sim \sqrt{T/m}$, so $D_s \sim v_\downarrow^2 \tau_\downarrow$ is not strongly polarization dependent for $T > T_{F\downarrow}$; the experimental results [1,2] are consistent with this. The heat, on the other hand, is mostly carried by the up atoms at high polarization, resulting in $D_T \sim D_s n_\uparrow/n_\downarrow$, a relation between the two diffusivities that appears to remain true at high polarization for all T away from the superfluid phases. At $p = 0$ and high T the two diffusivities are comparable, but D_T remains larger than D_s because a single s-wave scattering event completely randomizes the total spin current carried by the two atoms, while the component of the heat current carried by their center of mass is preserved. Thus, it appears that the heat mode always diffuses faster than the spin mode.

Moving towards lower T, let us next pause at $T = T_{F\uparrow}$, noting that here $v_\uparrow \sim v_\downarrow \sim \sqrt{T/m}$, and $\tau_\downarrow$ is the larger of $\frac{\hbar}{T}$ and $\frac{\hbar}{Tk_F^2a^2}$. For the polarized gas $\tau_\uparrow \sim \tau_\downarrow n_\uparrow/n_\downarrow$.

We next (still just power counting) look at the polarized gas in the intermediate temperature regime $T_{F\downarrow} < T < T_{F\uparrow}$, where the majority atoms are degenerate ($v_\uparrow \sim \sqrt{T_{F\uparrow}/m}$), while the minority atoms are not ($v_\downarrow \sim \sqrt{T/m}$). Some changes from the high-T regime are as follows: Only up atoms with energy within $\sim T$ of $T_{F\uparrow}$ are involved in the scattering and all but a fraction $T/T_{F\uparrow}$ of the final states of the scattering are Pauli-blocked due to the degeneracy of the up atoms. This increases $\tau_\downarrow$ by a factor of $(T_{F\uparrow}/T)^2$, and $\tau_\uparrow$ by a factor of $T_{F\uparrow}/T$, compared to their values at $T = T_{F\uparrow}$. Thus, $\tau_\downarrow$ is the larger of $\frac{\hbar}{T_{F\uparrow}}(\frac{T_{F\uparrow}}{T})^2$ and $\frac{\hbar}{T_{F\uparrow}k_{F\uparrow}^2a^2}(\frac{T_{F\uparrow}}{T})^2$. As a result, $D_s \sim v_\downarrow^2\tau_\downarrow$ is the larger of $\frac{\hbar T_{F\uparrow}}{mT}$ and $\frac{\hbar T_{F\uparrow}}{mTk_{F\uparrow}^2a^2}$, while D_T is again larger than D_s by a factor $n_\uparrow/n_\downarrow$. This estimate of D_s is consistent with a previous quantitative calculation [22,23]. Note that the temperature dependence of D_s crosses over from a decreasing function of T at low T to an increasing function at high T. The recent measurements [2] of the spin drag in a polarized unitary gas show this crossover occurring at roughly $T = 0.4T_{F\uparrow}$. On the BEC side of the Feshbach resonance, the minority atoms bind in to bosonic Feshbach molecules at low-enough T. However, as long as these molecules remain nondegenerate and thus not superfluid, the above estimates of the diffusivities should hold.

For $T < T_{F\downarrow}$, the minority atoms become degenerate. This leads to superfluidity on the BEC side of the Feshbach resonance as well as at low polarization near unitarity. However, there are regimes on the BCS side of the resonance as

well as near unitarity at high polarization where the minority atoms (near unitarity strongly "dressed" as polarons) form a degenerate Fermi gas. Here the important change from the intermediate temperature regime at the level of "power counting" is that only minority atoms with energy within $\sim T$ of $T_{F\downarrow}$ are involved in the scattering and they have momentum $k_{F\downarrow}$ instead of a thermal momentum. This increases the diffusivities by a factor of $T_{F\downarrow}/T$, so the spin diffusivity in these degenerate Fermi liquid regimes is the larger of $\frac{\hbar T_{F\uparrow} T_{F\downarrow}}{mT^2}$ and $\frac{\hbar T_{F\uparrow} T_{F\downarrow}}{mT^2 k_{F\uparrow}^2 a^2}$. We expect that D_T is still greater than D_s by a factor of $n_\uparrow/n_\downarrow$ but this question should be examined more carefully within Fermi liquid theory.

At low temperature, the polarized Fermi liquid may become a p-wave superfluid, with pairing within one species mediated by the attraction to the other species [24], or it may have a Fulde-Ferrell-Larkin-Ovchinnikov phase with Cooper pairs of nonzero total momentum [25–27]. In the superfluid phases, the thermal diffusivity should diverge to infinity, as heat is carried ballistically by second sound modes. The spin diffusivity presumably remains finite in the superfluid phases, although, as we discuss below, the spin Seebeck effect appears to generally be divergent in a polarized superfluid.

V. SPIN SEEBECK AND SPIN PELTIER EFFECTS

More challenging to estimate than these spin and thermal diffusivities are the effects that mix spin and heat transport, namely the spin Seebeck and the spin Peltier effects. Here we present "simple" arguments for the signs of these effects in two regimes: (1) far away from unitarity for all temperature ranges, and (2) at unitarity in the classical regime. Here we always consider a spin-polarized gas, since these "magnetocaloric" effects vanish by symmetry in the case of an unpolarized gas where the two species also have equal mass.

(1) Well away from unitarity ($|k_F a| \ll \min\{1, \sqrt{T_F/T}\}$), the scattering cross section is essentially a^2 and independent of momentum for all temperatures, since the interaction is weak and the atoms are not thermally excited to $\lambda < |a|$. Generally, the scattering rate is proportional to the *cross section* × *relative speed*. Thus, in this (low energy) regime, the scattering rate is $\sim a^2 |\mathbf{v}_\uparrow - \mathbf{v}_\downarrow|$. This implies minority atoms will scatter more frequently with the majority atoms of higher energy than majority atoms of lower energy since higher-energy majority atoms have higher relative speed. Consequently, the direction of the minority current is along the flow of higher-energy ("hot") majority atoms and thus parallel to the heat current. For a uniformly spin-polarized gas with a temperature gradient, where the spin Seebeck effect occurs, the primary current is the heat current transporting hot majority atoms from the hot region to the cold region and transporting "cold" majority atoms from the cold region to the hot region. The fact that the minority current is aligned with that of the hot majority atoms means the direction of the net spin current (spin Seebeck current) is opposite from that of the heat current. Thus, the initially cold region becomes less polarized due to minority atoms transported by the spin Seebeck current.

For a polarized gas with a polarization gradient but zero temperature gradient, where the spin Peltier effect occurs, the primary current is the spin current which transports minority atoms from the less-polarized region to the more-polarized region. Since again these minority atoms scatter more often with "hot" majority atoms, the resulting heat current is towards the more-polarized region, resulting in a spin Peltier (heat) current whose direction is opposite to the primary spin current. In summary, for a gas far from unitarity, the primary currents and the magnetocaloric currents are in opposite directions. In other words, the off-diagonal elements in Eq. (5) are negative while the diagonal elements are positive.

(2) At high temperatures ($T \gg T_{F\uparrow}$) and near unitarity ($|k_F a| \gg k_F \lambda > 1$), the s-wave scattering cross section is $1/(k_r/2)^2$ and thus is momentum-dependent, where $k_r = |\mathbf{k}_\uparrow - \mathbf{k}_\downarrow|$ is the relative momentum. Therefore, the scattering rate is roughly $\sim \frac{1}{k_r^2} \times v_r \sim \frac{1}{k_r}$. As a result, now minority atoms scatter more often with cold majority atoms. Since this is exactly the opposite from the case of far away from unitarity, the spin Seebeck and spin Peltier currents are reversed relative to the above discussion in (1). Therefore, at high temperature and unitarity, the primary currents and the magnetocaloric currents are in the same directions, giving S_s' in Eq. (5) positive sign. As we see in the next section, the spin Peltier coefficient P_s' in Eq. (5) is negative for low polarization and becomes positive for high polarization. This sign change in P_s' comes from the definition of currents and choice of driving forces and this is clarified in the Sec. VII, where we discuss the Kubo approach. Directions of the spin Seebeck effect in both limiting regimes are illustrated in Fig. 1.

At low temperatures and unitarity, it is not straightforward to apply the above argument to predict the direction of spin Seebeck and/or spin Peltier currents since the many-body effects may significantly modify the scattering cross section [28,29], which begins to depend on the center-of-mass momentum as well as the relative momentum. There is, however, a different line of argument that indicates that the sign of the spin Seebeck effect near unitarity remains the same as the temperature is lowered. Consider low-enough temperatures and polarization less than the Chandrasekhar-Clogston limit [30,31], in the superfluid phase [32,33]. When there is a temperature gradient in the system, heat flows "ballistically" from the hot region to the cold region by flow of the normal fluid with respect to the superfluid (in the usual two-fluid description of the superfluid phase). In the reference frame where the total particle density current vanishes (center-of-mass frame), the superfluid flows in the opposite direction to counterbalance the mass current of the normal fluid. Since the s-wave superfluid consists of equal numbers of majority and minority atoms, both the spin current and the heat current are carried only by the normal fluid. As a result, the spin Seebeck current and the heat current are in the same directions at low temperature in and, presumably, near the superfluid phase. Therefore, we expect the sign of the spin Seebeck effect to remain the same for all temperatures at unitarity. Both the thermal conductivity and the spin Seebeck coefficient will diverge at the transition to the superfluid phase.

As another approach to these questions, there is an interesting artificial interaction, namely the Maxwellian interaction where the scattering cross section is proportional to $1/v_r$ and the Boltzmann equation can be solved exactly in the high-temperature limit. Since the scattering rate does not depend on relative velocity [$(1/v_r) \times v_r =$ constant], there are no spin Seebeck or spin Peltier currents in this case.

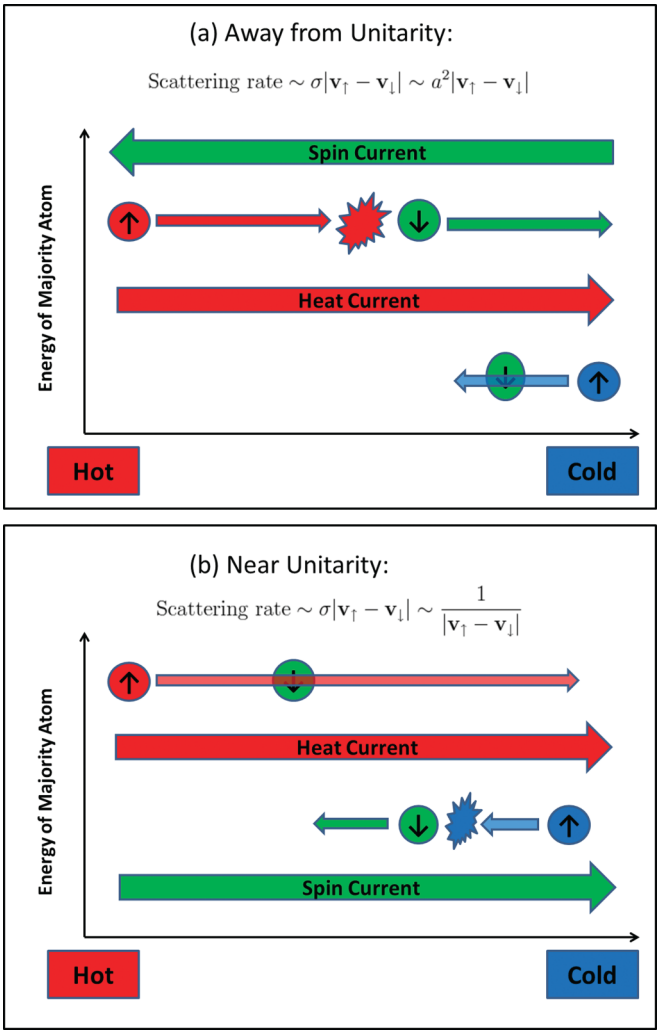

FIG. 1. (Color online) Illustration of the spin Seebeck effect. (a) Far away from unitarity, the scattering rate is proportional to the relative speed. Thus, "hot" majority (↑) atoms (top) collide more often with minority (↓) atoms than do "cold" majority atoms (bottom), giving the spin Seebeck current and the heat current opposite directions. (b) At unitarity, the scattering rate is inversely proportional to the relative speed. Therefore, the direction of the spin Seebeck current is reversed relative to (a).

Then, if we perturb the scattering cross section around the Maxwellian case, putting in an additional relative-velocity dependence to the scattering rate "by hand," we can perturbatively calculate the spin Seebeck and spin Peltier currents and manipulate the direction of these currents by changing the sign of the perturbation. This allows us to explicitly show how the magnetocaloric currents are generated from a relative-velocity-dependent cross section. This is discussed in the following section in detail.

VI. QUANTITATIVE APPROACH 1: THE BOLTZMANN EQUATION

A. Linearized Boltzmann equation and its scaling

In the limit of high temperature $T \gg T_F$, the gas is effectively classical, and its dynamics obey the Boltzmann equation. In the absence of external forces but with gradients in local temperature and local densities, the steady-state Boltzmann equation for species i ($i = \uparrow$ or $\downarrow$) is the following ($i \neq j$):

$$\frac{\hbar}{m}\mathbf{k}_i \cdot \nabla f_i = \int \frac{d^3\mathbf{k}_j}{(2\pi)^3} d\sigma \frac{\hbar|\mathbf{k}_\uparrow - \mathbf{k}_\downarrow|}{m} [f(\mathbf{k}'_\uparrow) f(\mathbf{k}'_\downarrow) - f(\mathbf{k}_\uparrow) f(\mathbf{k}_\downarrow)], \tag{6}$$

where $f(\mathbf{k}_i)$ is the momentum distribution of species i, and the velocity is $\mathbf{v}_i = \hbar\mathbf{k}_i/m$. $\mathbf{k}'_\uparrow$ and $\mathbf{k}'_\downarrow$ are momenta after collision and satisfy the energy momentum conservation. Working near equilibrium, we linearize the Boltzmann equation by introducing a small deviation ψ_i:

$$f_i = f_i^0(1 + \psi_i), \tag{7}$$

where f_i^0 is the equilibrium distribution. In this high-temperature regime, the equilibrium distribution is the Boltzmann distribution, $f_i^0(k) = n_i\lambda^3 \exp[-E(k)/T]$ and $E(k) = \frac{\hbar^2k^2}{2m}$. Since the most relevant length scale in the classical regime is the thermal de Broglie wavelength λ, it is convenient to scale the wave vector $\mathbf{k}$ with λ; $\mathbf{k} = \mathbf{q}/\lambda$. Then, $E(q)/T = \frac{q^2}{4\pi}$.

Let us impose the mechanical equilibrium condition. In this classical limit, it is enough to use the ideal gas pressure at equilibrium; $P = nT = (n_\uparrow + n_\downarrow)T$. From the spatially uniform pressure condition we can relate the density gradients and the temperature gradient via

$$\frac{\nabla n}{n} = -\frac{\nabla T}{T}, \tag{8}$$

to linear order in the gradients. This relation enables us to express the currents in terms of any two linearly independent "driving" terms such as $(\nabla n_\uparrow, \nabla n_\downarrow)$, $(\nabla T, n\nabla p)$, $(\nabla T, \nabla(\mu_\uparrow - \mu_\downarrow))$ or any other convenient combinations. It is convenient to work with $(\nabla n_\uparrow, \nabla n_\downarrow)$ in intermediate stages of the calculation and then transform it to the desired combination of driving forces using the equilibrium equation of state. Then the λ scaled linearized Boltzmann equations we need to solve become

$$\frac{1}{n_i}\nabla n_i \cdot \mathbf{q}_i - \frac{1}{n}\left(\frac{q_i^2}{4\pi} - \frac{3}{2}\right)\nabla n \cdot \mathbf{q}_i = n_j \int \frac{d^3\mathbf{q}_j}{(2\pi)^3} d\sigma e^{-q_j^2/4\pi} (\psi'_\uparrow + \psi'_\downarrow - \psi_\uparrow - \psi_\downarrow)|\mathbf{q}_\uparrow - \mathbf{q}_\downarrow|, \tag{9}$$

with $i \neq j$. ψ'_i takes $\mathbf{q}'_i$ as an argument.

We follow the standard definitions of the particle and energy currents of each species [34],

$$\mathbf{j}_i = \int \frac{d^3\mathbf{k}_i}{(2\pi)^3} f_i \mathbf{v}_i = n_i \int \frac{d^3\mathbf{q}_i}{(2\pi)^3} e^{-q_i^2/4\pi} \psi_i \frac{\hbar}{m}\frac{\mathbf{q}_i}{\lambda}, \tag{10}$$

$$\mathbf{j}_{\epsilon i} = \int \frac{d^3\mathbf{k}_i}{(2\pi)^3} f_i \mathbf{v}_i E_i = n_i \frac{T}{4\pi} \int \frac{d^3\mathbf{q}_i}{(2\pi)^3} e^{-q_i^2/4\pi} \psi_i \frac{\hbar}{m}\frac{q_i^2\mathbf{q}_i}{\lambda}. \tag{11}$$

Because of Galilean invariance, we need to specify an inertial frame. Except when specified otherwise, we work in the frame where the local particle current is zero: $\mathbf{j}_n = \mathbf{0}$.

B. Approximate solution

The s-wave scattering cross section that captures most physics of a short-range interaction is

$$\frac{d\sigma}{d\Omega} = \frac{a^2}{1+\left(\frac{k_r a}{2}\right)^2} = \lambda^2 \frac{(a/\lambda)^2}{1+\left(\frac{q_r a}{2\lambda}\right)^2}, \tag{12}$$

where we scaled the scattering length a with λ. An exact solution of the Boltzmann equation for such a cross section is not known and thus we need to resort to approximation methods. One of the standard ways to find an approximate solution of a linearized Boltzmann equation is the moment expansion method (for example, see [35]). Considering all symmetries and assuming the true solution is analytic near small $\mathbf{q}$, we take the following ansatz for ψ_i ($i = \uparrow, \downarrow$):

$$\psi_i = -\lambda \sum_{j=\uparrow,\downarrow} \sum_{\ell=0}^{L} C_{\ell ij} q_i^{2\ell} \frac{\nabla n_j \cdot \mathbf{q}_i}{n_j}. \tag{13}$$

We only consider the case where $\nabla n_\uparrow$ and $\nabla n_\downarrow$ are both parallel to the z axis. We need to determine the dimensionless coefficients $\{C_{\ell ij}\}$.

The procedure to obtain an approximate solution of the Boltzmann equation is the following: First, insert the above ansatz into the right-hand side of Eq. (9). Then multiply both sides of Eq. (9) by $q_i^{2\ell} q_{iz} \frac{1}{(2\pi)^3} \exp[-q_i^2/4\pi]$ ($\ell = 0,1,2,\ldots,L$) and integrate out all momenta. Matching coefficients of density gradients gives $4(L+1)$ linear equations for the $\{C_{\ell ij}\}$, all of which, however, are not linearly independent due to Galilean invariance. We need to fix the reference frame to uniquely determine a solution. Once we choose an appropriate reference frame (usually $\mathbf{j}_\uparrow + \mathbf{j}_\downarrow = 0$), we have $4(L+1)$ linearly independent equations for the $\{C_{\ell ij}\}$. Determining the $\{C_{\ell ij}\}$, we have an approximate solution to the Boltzmann equation, that is, an approximate momentum distribution from which we can calculate all currents of interest. Here we present results of two limiting cases, far away from unitarity ($\frac{d\sigma}{d\Omega} = a^2$) and at unitarity ($\frac{d\sigma}{d\Omega} = \frac{4}{k_r^2}$), which allow an analytic solution (of this approximation) without special functions. These correspond to the two limits $\lambda/|a| \gg 1$ and $\lambda/|a| \ll 1$, respectively. For a general scattering length a, it is still possible to find a closed-form expression in terms of exponential integrals and incomplete Γ functions whose arguments depend on $\lambda/|a|$.

Obtaining $C_{\ell ij}$ from a straightforward calculation in the $\mathbf{j}_\uparrow + \mathbf{j}_\downarrow = 0$ frame, we can express the heat current and spin current in terms of $\nabla n_\uparrow$ and $\nabla n_\downarrow$. Here we choose to express final results in the format of Eq. (5) since we want to study the spin Seebeck coefficient S_s' in detail, which could be the most directly accessible signature of the spin Seebeck effect in experiments. Therefore, we transform these two gradients to ∇T and $n\nabla p$, using the equilibrium equation of state and the mechanical equilibrium condition. The transformation matrix is

$$\begin{pmatrix} \nabla n_\uparrow \\ \nabla n_\downarrow \end{pmatrix} = \begin{pmatrix} -\frac{T}{n} & -\frac{T}{n} \\ \frac{2n_\downarrow}{n} & -\frac{2n_\uparrow}{n} \end{pmatrix}^{-1} \begin{pmatrix} \nabla T \\ n\nabla p \end{pmatrix}. \tag{14}$$

Since the left-hand side of Eq. (9) is a third-order polynomial in q, the simplest ansatz is with $L = 1$. In principle, we can go up to any order in L we want, but an $L \geqslant 2$ ansatz complicates the computation, while the simplest ansatz already exhibits nontrivial results. Furthermore, we find that the change in S_s' on moving from the $L = 1$ to the $L = 2$ approximation is quite small: about a 1% change near unitarity and in the value of $\lambda/|a|$ at the zero crossing, growing to near 7% far from unitarity. Therefore, here we only present results of $L = 1$.

We present our results in the conventional format (without λ scaling): Near unitarity ($|a| \gg \lambda$),

$$\begin{pmatrix} \mathbf{j}_{\text{heat}} \\ \mathbf{j}_{\text{spin}} \end{pmatrix} = -\frac{45\pi^{3/2}}{608\sqrt{2}} \left[\frac{\hbar}{m}\left(\frac{T}{T_F}\right)^{3/2}\right] \begin{pmatrix} \kappa_u' & \frac{1}{2}\frac{(n_\uparrow - n_\downarrow)Tn}{n_\uparrow n_\downarrow} - \frac{39}{10} T \ln\left(\frac{n_\uparrow}{n_\downarrow}\right) \\ \frac{(n_\uparrow - n_\downarrow)}{T} & \frac{39}{10} \end{pmatrix} \begin{pmatrix} \nabla T \\ n\nabla p \end{pmatrix}, \tag{15}$$

where κ_u' (proportional to the thermal conductivity at unitarity) is

$$\kappa_u' = \frac{5}{16} n \left(\frac{(73n_\uparrow^2 + 82 n_\uparrow n_\downarrow + 73 n_\downarrow^2)}{n_\uparrow n_\downarrow}\right) - (n_\uparrow - n_\downarrow) \ln\left(\frac{n_\uparrow}{n_\downarrow}\right). \tag{16}$$

Far away from unitarity ($|a| \ll \lambda$),

$$\begin{pmatrix} \mathbf{j}_{\text{heat}} \\ \mathbf{j}_{\text{spin}} \end{pmatrix} = -\frac{15\pi^{3/2}}{224\sqrt{2}} \left(\frac{\hbar}{m(k_F a)^2}\sqrt{\frac{T}{T_F}}\right) \begin{pmatrix} \kappa_a' & -\frac{1}{2}\frac{(n_\uparrow - n_\downarrow)Tn}{n_\uparrow n_\downarrow} - \frac{43}{10} T \ln\left(\frac{n_\uparrow}{n_\downarrow}\right) \\ -\frac{(n_\uparrow - n_\downarrow)}{T} & \frac{43}{10} \end{pmatrix} \begin{pmatrix} \nabla T \\ n\nabla p \end{pmatrix}, \tag{17}$$

where κ_a' (proportional to the thermal conductivity far away from unitarity) is

$$\kappa_a' = \frac{5}{8} n \left(\frac{(29n_\uparrow^2 + 26 n_\uparrow n_\downarrow + 29 n_\downarrow^2)}{n_\uparrow n_\downarrow}\right) + (n_\uparrow - n_\downarrow) \ln\left(\frac{n_\uparrow}{n_\downarrow}\right). \tag{18}$$

The above matrices clearly exhibit the existence of the spin Seebeck and spin Peltier effects (nonvanishing off diagonal terms) only for nonzero polarization. We mostly focus now on the spin Seebeck coefficient S_s', which gives the spin current due to a temperature gradient in the absence of a spin polarization gradient.

As argued in the previous section, the spin Seebeck coefficient changes sign as a function of interaction strength. Near unitarity [Eq. (15)], it is positive so the spin Seebeck current and the heat current are in the same direction. Far away from unitarity [Eq. (17)], it is negative so the spin Seebeck current and the heat current are in the opposite direction.

Next let us consider the polarization dependence of the transport coefficients. The heat current and the temperature gradient are even under spin index exchange while the spin current and the polarization gradient are odd. Therefore, thermal conductivity and spin diffusivity are even functions of polarization while magnetocaloric effects are odd functions of polarization. The above matrices satisfy these polarization parity constraints and the form of the polarization dependence of the transport coefficients is the same in both limits of large and small $\lambda/|a|$. In fact, we can show that the polarization dependence (thus, $n_\uparrow$ and $n_\downarrow$ dependence) of the transport coefficients maintains this form for all values of $\lambda/|a|$ and to all orders of approximation. The proof is given in Appendix A. Here we study the Seebeck coefficient S_s' in detail, which is our prime interest.

Although it is conventional to scale the scattering length a with k_F (as we did in the above matrices), it is easier to see the structure of the Seebeck coefficient in terms of $\lambda/|a|$ in the classical regime. Once we obtain an approximate solution of the Boltzmann equation with a general $\lambda/|a|$ and $L = 1$, we can explicitly show that

$$S_s' = \frac{\hbar}{m}\frac{n_\uparrow - n_\downarrow}{n\lambda^3}\frac{1}{T}h_1(\lambda/|a|), \tag{19}$$

where $h_1(x)$ is a dimensionless function that contains $Ei(x)$, the exponential integral, and diverges as $\lambda/|a| \to \infty$ [see Eq. (17)]. Since it contains no explicit temperature or polarization dependence, $h_1(x)$ is independent of polarization and temperature at this order of approximation ($L = 1$). Therefore, once we scale the scattering length by λ and factor out dimensionful parameters and polarization, the dependence of S_s' on the scattering length is determined by $h_1(x)$ and the value of $\lambda/|a|$ at which S_s' crosses zero is solely determined by the equation $h_1(x) = 0$, which is independent of temperature and polarization. In the $L = 1$ approximation, the zero-crossing value is $\lambda/|a| \simeq 3.62$. Figure 2 is a plot of the normalized S_s' as a function of $\lambda/|a|$. In the $L = 2$ approximation, we find that the scaling function $h_1(x)$ slightly changes to $h_2(x)$ and the zero-crossing point remains at $\lambda/|a| \simeq 3.62$. In Appendix A, we show that the structure of Eq. (19) (and other transport coefficients in a similar manner) remains to all orders of approximation. Therefore, we may conclude that in this classical regime the Seebeck coefficient is linearly proportional to the polarization p and inversely proportional to $T\lambda^3$, once we scale the scattering length by λ.

Note that Eqs. (15) and (17) do not explicitly satisfy the Onsager relation and the spin Peltier coefficient P_s' is still negative for low polarization even near unitarity. These

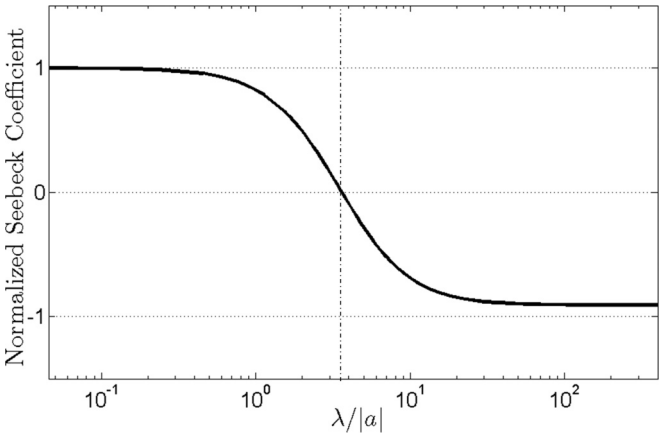

FIG. 2. Normalized Seebeck coefficient S_s' as a function of $\lambda/|a|$ in the classical regime. The normalization is by a factor of $\frac{15}{608\sqrt{2}}(\frac{\hbar}{m}\frac{1}{T\lambda^3}\frac{1+4\pi(a/\lambda)^2}{(a/\lambda)^2})\frac{(n_\uparrow - n_\downarrow)}{n}$. This choice of normalization, which is inversely proportional to a typical value of scattering cross section with scaled scattering length a/λ, gives finite values at both limits and gives the Seebeck coefficient 1 at unitarity [Eq. (15)]. We can see that S_s' changes sign near $\lambda/|a| \simeq 3.62$. Since we factored out all explicit temperature and polarization dependence in the normalization choice and scaled the scattering length, this plot remains the same for all temperature and polarization ranges at this order of approximation ($L = 1$).

come from the definition of diffusive currents and choice of representation and are discussed in detail in the next section in terms of the Kubo formula. For now, we focus on the spin Seebeck coefficient S_s' which appears to be the most promising candidate of the magnetocaloric effects to be detected in experiments.

From the Einstein relation, we obtain the thermal diffusivity D_T after dividing κ_u' and κ_a' by $C_P = 5n/2$, the heat capacity per volume at fixed pressure and polarization. These results confirm the "power-counting" estimates of diffusivities: In case of an unpolarized gas ($n_\uparrow = n_\downarrow$), D_s at unitarity is $\cong 1.1\frac{\hbar}{m}(\frac{T}{T_F})^{3/2}$, which is consistent with previous work [1,21]. Also, the thermal diffusivity does satisfy the inequality, $D_T > D_s$, at zero polarization. Furthermore, for a highly polarized gas ($n_\uparrow \gg n_\downarrow$), $D_T \sim \frac{n^2}{n_\uparrow n_\downarrow}D_s \sim \frac{n_\uparrow}{n_\downarrow}D_s$, which is also as expected from the "power-counting" estimates.

C. Estimate of the spin Seebeck effect

The spin Seebeck effect seems to be more accessible to experiment than the spin Peltier effect, since the measurement of spin currents has already been done [1,2] and seems more straightforward than measuring heat currents. Also, the spin mode diffuses slower than the heat mode, so the change in spin polarization produced by the spin Seebeck effect will relax slowly, enhancing its detectability. An initially fully equilibrated spin-polarized gas could be heated at one end, producing a temperature gradient, and then the resulting spin current could be measured if it is large enough.

Let us make quantitative estimates of signatures of the spin Seebeck effect that are relevant to such a proposed experiment. We make our estimates for a gas in a uniform potential, but the results should be roughly correct for a gas

cloud in a trap if one compares points at opposite ends of the cloud that are at the same potential so will have the same local densities and polarization at equilibrium. First, apply a small, long-wavelength temperature inhomogeneity along the z axis. In mechanical equilibrium, nonuniform temperature implies nonuniform total density [by Eq. (8)], thus temperature modulation implies density modulation. This enables us to write the initial total density as

$$n(t=0,z) = n_0 + \delta n_0 \cos wz, \tag{20}$$

where w $(=\pi/L)$ is the wave number of the modulation, L is the length of the system over which the full temperature difference is applied, and δn_0 is the small deviation of total density from the mean value n_0 due to this temperature difference (at uniform pressure). Equation (8) implies that if we initially locally heat $z = L$ relative to $z = 0$, then this location initially has lower density because of thermal expansion. From the initial condition of uniform polarization, the density of each spin component at $t = 0$ is

$$n_i(t=0,z) = n_{i0} + \delta n_{i0} \cos wz, \tag{21}$$

$$\delta n_{i0} = \frac{n_{i0}}{n_0}\delta n_0. \tag{22}$$

Then, we write a diffusion matrix in the form of Eq. (1), assuming that there are only these diffusive currents (no initial other motion of the gas).

As mentioned above in Sec. III, the diffusion matrix has two eigenmodes, the spin mode with the eigenvalue $\mathfrak{D}_s$ and the thermal mode with the eigenvalue $\mathfrak{D}_T$. Applying the continuity equation to the diffusion matrix, we obtain a coupled set of heat equations with appropriate initial conditions, which can be solved immediately for $t > 0$ in terms of the two eigenmodes. The solution of the heat equation gives us the space-time dependence of density of each species:

$$\begin{pmatrix} n_\uparrow(t,z) \\ n_\downarrow(t,z) \end{pmatrix} = \begin{pmatrix} n_{\uparrow 0} \\ n_{\downarrow 0} \end{pmatrix} + \alpha e^{-\mathfrak{D}_s w^2 t}\delta n_{\downarrow 0}\begin{pmatrix} \gamma \\ 1 \end{pmatrix}\cos wz + \beta e^{-\mathfrak{D}_T w^2 t}\delta n_{\downarrow 0}\begin{pmatrix} \zeta \\ 1 \end{pmatrix}\cos wz, \tag{23}$$

where α,β,γ, and ζ are determined by initial conditions. See Appendix B for details. Since $\mathfrak{D}_T > \mathfrak{D}_s > 0$, the two diffusive modes relax to global equilibrium at different rates. At nonzero polarization, $|\gamma|,|\zeta| \neq 1$. From these two properties, the density deviations of each species have different time evolution from one another: The density deviation of one species relaxes nonmonotonically while the density of the other species relaxes monotonically. This nonmonotonic relaxation of density deviation is a qualitative signature of the spin Seebeck effect. Near unitarity, we already know that the heat current and the spin current due to a temperature gradient are in the same direction. Therefore, the initially colder region $(z < \pi/2w)$ becomes more polarized due to the spin Seebeck current. It turns out that the minority density deviation changes sign as it relaxes towards equilibrium. Far from unitarity, on the other hand, the initially cold region becomes less polarized, since the direction of the spin current is reversed, resulting in nonmonotonic relaxation of the majority density deviation. Figures 3 and 4 are plots of relaxation of the density deviations

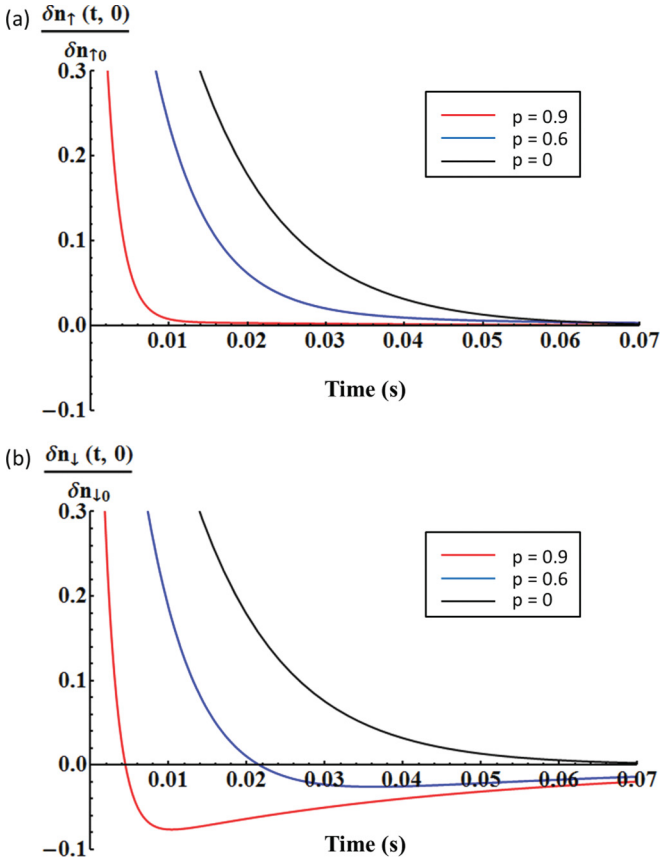

FIG. 3. (Color online) $\delta n_i(t,0)$ normalized by initial deviation δn_{i0} as a function of time near unitarity. (a) Majority density deviation relaxes monotonically for any polarization. (b) Minority density deviation shows nonmonotonic relaxation for $p > 0$ due to the spin Seebeck effect. Here we assume ^{6}Li atoms with $T/T_F = 4$ and the longitudinal length of the trap $L = 200$ μm to set the time scale. p increases from top to bottom.

of each species as a function of time for the two cases of near unitarity and of far away from unitarity.

Another consequence of the spin Seebeck effect is the change in polarization. As argued, the sign of the local polarization change depends on the direction of the spin Seebeck current. Figure 5 shows the (normalized) deviation of polarization from the average value as a function of time at $z = 0$. As expected, deviation is positive near unitarity and is negative far away from unitarity.

Perhaps one of the most easily accessible quantities in experiment is the density deviation of the species that shows nonmonotonic relaxation vs time. A dimensionless measure of the extremum deviation is $|\frac{\delta n_i(t_{i,\mathrm{ext}},0)}{\delta n_{i0}}|$, where $i = \uparrow$ away from unitarity and $i = \downarrow$ near unitarity and $t_{i,\mathrm{ext}}$ is the time when density deviation of species i is its extremum of opposite sign from the initial condition. Figure 6 shows the dimensionless measure of the extremum density deviation as a function of polarization. Near unitarity (solid line), it is a monotonically increasing function of polarization for $p < 1$ (at $p = 1$, $n_\downarrow$ is zero so the deviation of $n_\downarrow$ is undefined). Around $p \approx 0.8$, the strength of the spin Seebeck effect by this measure is about 5%. Far from unitarity (dashed line), this signal is much weaker. This is expected since the spin Seebeck effect is a consequence

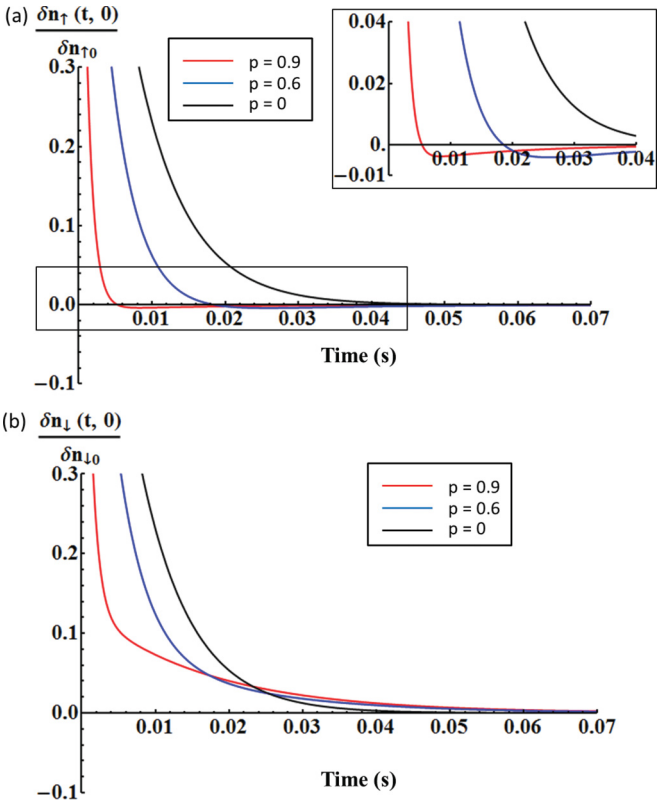

FIG. 4. (Color online) $\delta n_i(t,0)$ normalized by initial deviation δn_{i0} as a function of time far away from unitarity. (a) Majority density deviation relaxes nonmonotonically for $p > 0$ due to the spin Seebeck effect. Inset figure magnifies the nonmonotonic part of majority density deviations which are very weak compared to the minority density deviations at unitarity shown in Fig. 3. (b) Minority density deviation relaxes monotonically for any polarization. Here we assume ^{6}Li atoms with $T/T_F = 4$ and $\lambda/|a| = 4$ and the longitudinal length of the trap $L = 200$ μm to set the time scale.

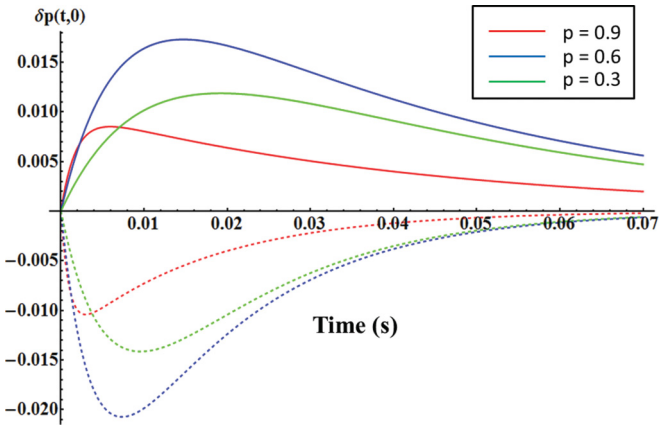

FIG. 5. (Color online) Normalized polarization deviation as a function of time for three global polarization values, $p = 0.9$ (lower curve), 0.6 (highest curve), and 0.3 (center curve). Near unitarity (solid lines) the polarization deviation is positive while far away from unitarity (dashed lines) it is negative. We found that the polarization deviation is the largest near $p = 0.6$ in both limits. Same physical parameters as Figs. 3 and 4 were used to fix the time scale. The polarization deviation $\delta p(t,0)$ at the initially cold end of the cloud is normalized by the initial total density deviation, $\delta n_0/n_0$.

of interaction and does not exist in the noninteracting gas. Thus, the spin Seebeck effect should be strongest near unitarity. Note that in both limits, the spin Seebeck effect disappears when the gas is unpolarized, $p = 0$.

The spin Seebeck effect is a small effect. In the regimes where we have been able to estimate it and using the measures we have been able to devise, it is less than a 10% effect. However, it is worth emphasizing that these computations are done in the classical regime, so the spin Seebeck effect does not demand extremely low temperatures to detect it. We expect it to be most readily detected at temperatures of order T_F, where the diffusivities are minimized so the resulting time scales are longest. In addition, the procedure to detect it discussed in this section does not require knowledge of the system's equation of state. Importantly, we propose a type of experiment where the the spin Seebeck effect is a *qualitative effect*, namely a nonmonotonicity of the system's relaxation to global equilibrium.

D. Exactly solvable model

So far, our approach was based on an approximation method. Therefore, it is worthwhile to compare the main findings to a different approach, namely perturbing around the Maxwellian model, where the scattering cross section is inversely proportional of the relative speed [9]. The linearized Boltzmann equation can be exactly solved for the classical Maxwellian model.

Let us recall the argument from which we determined directions of the magnetocaloric effects. Since the scattering rate is proportional to the product of the cross section and relative speed, the scattering rate is independent of momentum for the Maxwellian interaction. Therefore, we expect that $S_s' = 0$ for any polarization. It is straightforward to exactly

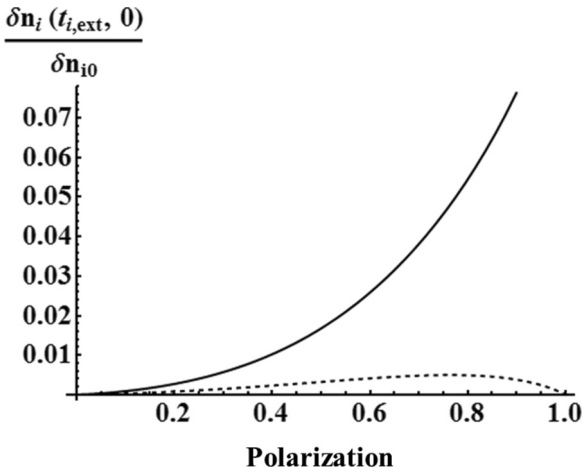

FIG. 6. Extremum density deviation normalized by initial deviation, $|\frac{\delta n_i(t_{i,\mathrm{ext}},0)}{\delta n_{i0}}|$ as a function of polarization. Near unitarity (solid line), $i = \downarrow$; far from unitarity (dashed line), $i = \uparrow$. $t_{i,\mathrm{ext}}$ is the time when the density deviation of species i reaches its extremum. Far from unitarity (dashed line), the normalized extremum density deviation vanishes in the high polarization limit since there are no minority atoms to scatter from.

solve the Boltzmann equation using the ansatz Eq. (13) with $L = 1$ to confirm this.

The next step is to perturb the Maxwellian scattering cross section to generate magnetocaloric currents. One simple way to perturb the cross section is to add a small term which depends linearly on relative momentum to the original cross section:

$$\frac{d\sigma}{d\Omega} = S_0\left(\frac{1}{k_r} + \epsilon k_r\right), \tag{24}$$

where S_0 is a constant of the dimension of length and ϵ is a small expansion parameter. For a positive ϵ, the momentum dependence of the scattering rate is similar to the case away from unitarity, higher scattering rate for higher relative momentum. Thus, we expect the resulting spin Seebeck current is in the opposite direction from the primary heat current. For a negative ϵ, the momentum dependence resembles the case near unitarity and therefore we expect the resulting spin Seebeck current is in the same direction as the primary heat current.

To find the solution of the Boltzmann equation up to linear order in ϵ, we need $L = 2$ in the ansatz of Eq. (13). After a straightforward calculation, we obtain the following results:

$$\begin{pmatrix}\mathbf{j}_{\text{heat}}\\ \mathbf{j}_{\text{spin}}\end{pmatrix} = -D_0\begin{pmatrix}\kappa_M' & -\frac{\pi\epsilon(n_\uparrow-n_\downarrow)Tn}{2n_\uparrow n_\downarrow\lambda^2} - \frac{T}{10}\left(1-\frac{20\pi\epsilon}{\lambda^2}\right)\ln\left(\frac{n_\uparrow}{n_\downarrow}\right)\\ -\frac{\pi\epsilon(n_\uparrow-n_\downarrow)}{\lambda^2 T} & \frac{1}{10}\left(1-\frac{20\pi\epsilon}{\lambda^2}\right)\end{pmatrix}\begin{pmatrix}\nabla T\\ n\nabla p\end{pmatrix}, \tag{25}$$

where κ_M' (proportional to the thermal conductivity of the Maxwellian model) is

$$\kappa_M' = \frac{1}{2}n\left(\frac{(n_\uparrow^2 + n_\uparrow n_\downarrow + n_\downarrow^2)}{n_\uparrow n_\downarrow} - \frac{3\pi\epsilon}{\lambda^2}\frac{(9n_\uparrow^2 + 10n_\uparrow n_\downarrow + 9n_\downarrow^2)}{n_\uparrow n_\downarrow}\right) + \frac{\pi\epsilon(n_\uparrow - n_\downarrow)}{\lambda^2}\ln\left(\frac{n_\uparrow}{n_\downarrow}\right). \tag{26}$$

D_0 is $\frac{5\hbar}{mS_0 n\lambda^2}$, with units of a diffusivity.

We immediately see that all off-diagonal elements vanish for zero polarization. When $\epsilon = 0$, we see that $S_s' = 0$ and thus we conclude that the spin Seebeck effect is a consequence of momentum dependence of the scattering rate. The sign of the spin Seebeck current at nonzero ϵ is as expected. For P_s', we again see the logarithmic term which is discussed in the following section. Perturbing the Maxwellian scattering cross section reconfirms the sign argument for the spin Seebeck effect that we presented in the previous section.

VII. STRUCTURE OF TRANSPORT COEFFICIENTS: KUBO FORMULA

The Kubo formula gives a formally exact expression for the transport coefficients in the linear response regime (see, e.g., [36,37]). For irreversible processes in the linear response regime, what the the Kubo formula gives are the transport coefficients for the dissipative forces and currents associated with the entropy production. At mechanical equilibrium for our two-species gas, the dissipative forces are ∇T and $\nabla(\mu_\uparrow - \mu_\downarrow)$ [20]; thus, what we obtain from the Kubo formula is the diffusion matrix in the form of Eq. (2), whose off-diagonal terms always satisfy the Onsager relation. Thus, the diffusion matrix in the form of Eq. (5), in which we summarized the results in the previous section, does not generally satisfy the Onsager relation, although it is possibly easier to observe experimentally. In Appendix A, we summarize the results in the form of Eq. (2) and explicitly show both our approximate solutions and the perturbative solution from the exactly solvable Maxwellian model indeed satisfy the Onsager relation.

Following Ref. [36] and from Eq. (2), the spin Seebeck coefficient S_s and Peltier coefficient P_s can be expressed via the Kubo formula as

$$TS_s = \frac{1}{3VT}\int_0^\infty dt\,\langle \mathbf{J}_{\text{heat}}(0)\cdot\mathbf{J}_{\text{spin}}(t)\rangle \tag{27a}$$

$$= \frac{1}{3VT}\int_0^\infty dt\,\langle \mathbf{J}_{\text{heat}}(t)\cdot\mathbf{J}_{\text{spin}}(0)\rangle = P_s, \tag{27b}$$

where V is the total volume of the system and the current $\mathbf{J}$ is the volume integral of local current density,

$$\mathbf{J}(t) = \int d^3\mathbf{x}\,\mathbf{j}(\mathbf{x},t). \tag{28}$$

The average is taken over the equilibrium distribution, which is just the Boltzmann distribution of each species in the high-temperature classical regime.

Since we assume Galilean invariance, the total momentum of the entire gas is conserved. Therefore, any physical quantity which is transported with the total particle current $\mathbf{J}_n$ remains finite for all time t and gives a divergent contribution in the Kubo formula, meaning that quantity moves ballistically rather than diffusively. Therefore, it is crucial to use the frame-independent definition of the local diffusive currents from Eqs. (3) and (4). Let us write them again and slightly manipulate the heat current:

$$\mathbf{j}_{\text{spin}} = \frac{n_\downarrow}{n}\mathbf{j}_\uparrow - \frac{n_\uparrow}{n}\mathbf{j}_\downarrow, \tag{29}$$

$$\mathbf{j}_{\text{heat}} = \mathbf{j}_\epsilon - \mu_\uparrow\mathbf{j}_\uparrow - \mu_\downarrow\mathbf{j}_\downarrow - sT\mathbf{j}_n$$

$$= \mathbf{j}_\epsilon - \frac{5}{2}T\mathbf{j}_n - (\mu_\uparrow - \mu_\downarrow)\mathbf{j}_{\text{spin}}, \tag{30}$$

where $sT = \frac{5}{2}T - \frac{n_\uparrow}{n}\mu_\uparrow - \frac{n_\downarrow}{n}\mu_\downarrow$ and $\mathbf{j}_\epsilon = \mathbf{j}_{\epsilon\uparrow} + \mathbf{j}_{\epsilon\downarrow}$. Defining $\tilde{\mathbf{j}}_{\text{heat}} \equiv \mathbf{j}_\epsilon - (5T/2)\mathbf{j}_n$ [38], the Kubo formula gives us the

following spin Seebeck coefficient:

$$TS_s = P_s = \frac{1}{3VT}\int_0^\infty dt[\langle \tilde{\mathbf{J}}_{\rm heat}(0)\cdot \mathbf{J}_{\rm spin}(t)\rangle - (\mu_\uparrow - \mu_\downarrow)\langle \mathbf{J}_{\rm spin}(0)\cdot \mathbf{J}_{\rm spin}(t)\rangle] \quad (31)$$

$$= \frac{1}{3VT}\int_0^\infty dt\langle \tilde{\mathbf{J}}_{\rm heat}(0)\cdot \mathbf{J}_{\rm spin}(t)\rangle - T\ln\left(\frac{n_\uparrow}{n_\downarrow}\right)\sigma_s, \quad (32)$$

where σ_s is the spin conductivity given in Eq. (2) and $\mu_\uparrow - \mu_\downarrow = T\ln(n_\uparrow/n_\downarrow)$. Therefore, in this representation, the spin Seebeck coefficient (and thus also the spin Peltier coefficient) always carries an additional term of the spin conductivity σ_s multiplied by $-\ln(n_\uparrow/n_\downarrow)$. This is the origin of that term in P_s' in Eqs. (15), (17), and (25). We can understand the reason why the spin Seebeck coefficient S_s' does not include such a term from the following observation: At mechanical equilibrium and high temperature, we have

$$\nabla(\mu_\uparrow - \mu_\downarrow) = \ln\left(\frac{n_\uparrow}{n_\downarrow}\right)\nabla T + T\frac{n^2}{2n_\uparrow n_\downarrow}\nabla p. \quad (33)$$

Therefore, that $\nabla p = 0$ implies $\nabla(\mu_\uparrow - \mu_\downarrow) = \ln(n_\uparrow/n_\downarrow)\nabla T$. The spin current now becomes

$$\mathbf{j}_{\rm spin} = -\sigma_s\nabla(\mu_\uparrow - \mu_\downarrow) - S_s\nabla T \quad (34a)$$

$$= -D_s n\nabla p - \left[\sigma_s\ln(n_\uparrow/n_\downarrow) + S_s\right]\nabla T \quad (34b)$$

$$= -D_s n\nabla p - S_s'\nabla T. \quad (34c)$$

Thus, the additional $\sim\ln(n_\uparrow/n_\downarrow)$ term from Eq. (33) exactly cancels the similar term from Eq. (32). Consequently, what we have computed for S_s' in the previous section is the first term in Eq. (32) to which the sign argument in section IV should be applied.

We can extract more information from Eq. (30). In $\mathbf{j}_n = 0$ frame, the heat current is $\mathbf{j}_{\rm heat} = \mathbf{j}_\epsilon - T\ln(n_\uparrow/n_\downarrow)\mathbf{j}_{\rm spin}$. Thus, heat conductivity and spin Peltier coefficient always have contributions coming from spin current. Therefore, in the format of Eq. (5) we can write

$$\kappa' = \kappa_1' - T\ln(n_\uparrow/n_\downarrow)S_s', \quad (35)$$

$$P_s' = P_{s1}' - T\ln(n_\uparrow/n_\downarrow)D_s, \quad (36)$$

where κ_1' and P_{s1}' are first terms which do not originate from spin current. Results in the previous section clearly show this.

Last, we study the thermal conductivity, κ, in Eq. (2):

$$\kappa = \frac{1}{3VT^2}\int_0^\infty dt\langle \mathbf{J}_{\rm heat}(t)\cdot \mathbf{J}_{\rm heat}(0)\rangle \quad (37)$$

$$= \frac{1}{3VT^2}\int_0^\infty dt\langle \tilde{\mathbf{J}}_{\rm heat}(t)\cdot \tilde{\mathbf{J}}_{\rm heat}(0)\rangle - 2T\ln\left(\frac{n_\uparrow}{n_\downarrow}\right)S_s' + T\left[\ln\left(\frac{n_\uparrow}{n_\downarrow}\right)\right]^2\sigma_s. \quad (38)$$

The above structure of thermal conductivity is explicitly shown in Appendix C.

VIII. CONCLUSION AND OUTLOOK

We have studied diffusive spin and heat transport in a two-species atomic Fermi gas with short-range interaction at general polarization, temperature and scattering length. Using power counting, we first estimated the spin and thermal diffusivities in all regimes. We suggested a method to measure the thermal diffusivity, which has not yet been experimentally measured.

Our main focus was on the magnetocaloric effects, namely the spin Seebeck and spin Peltier effects. Observing the connection between the interaction strength and the dependence of the scattering rate on the relative momentum of two atoms, we were able to develop a qualitative argument for the signs of magnetocaloric effects. Near unitarity, magnetocaloric currents are in the same direction as the "primary" spin and heat currents, while their directions are reversed as we move to far away from unitarity. We then quantitatively estimated diffusivities and magnetocaloric effects in the classical regime using approximate solutions of the Boltzmann kinetic equation, thereby confirming the power-counting estimates of diffusivities and the sign argument for the magnetocaloric effects. We also proved the scaling of the transport coefficients is robust to all orders of approximation, in Appendix A.

Remaining in the classical regime, we proposed an experimental procedure to detect the spin Seebeck effect as a qualitative effect: a nonmonotonic relaxation towards equilibrium. This method is nice in that it does not require knowledge of the equation of state of the gas. In order to confirm these results and obtain a better understanding of the origin of these magnetocaloric effects, we also performed a controlled perturbation to the exactly solvable Maxwellian model. This approach agrees well with the approximate solutions of the Boltzmann equation.

To obtain the corresponding transport behavior quantitatively in the quantum degenerate (but normal) regime, we need spin-polarized Fermi liquid theory. We hope to report on this soon in a forthcoming paper.

ACKNOWLEDGMENTS

We thank Randy Hulet, Junehyuk Jung, Charles Mathy, Marco Schiro, Ariel Sommer, Henk Stoof, and Martin Zwierlein for helpful discussions. This work is supported by ARO Award No. W911NF-07-1-0464 with funds from the DARPA OLE Program. H.K. is partially supported by the Samsung Scholarship and the NSF (Grant No. DMR-0844115).

APPENDIX A: APPROXIMATE SOLUTION OF BOLTZMANN EQUATION TO ALL ORDERS

1. κ' and S_s'

First let us consider κ' and S_s' when $\nabla p = 0$. Observe that $\nabla p = 0$ and mechanical equilibrium condition imply

$$\frac{\nabla n_\uparrow}{n_\uparrow} = \frac{\nabla n_\downarrow}{n_\downarrow} = \frac{\nabla n}{n} = -\frac{\nabla T}{T}. \quad (A1)$$

Therefore, Eq. (13) simplifies to

$$\psi_i = \lambda \sum_{\ell=0}^{L} C_{\ell i} q_i^{2\ell} \frac{\mathbf{q}_i \cdot \nabla T}{T}, \tag{A2}$$

where we abbreviated $C_{\ell ii} + C_{\ell ij} \equiv C_{\ell i}$. Following the procedure explained in the main text, we can obtain the following set of linearly independent equations ($m = 1,2,\ldots,L$):

$$n_\uparrow \lambda^3 [\beta_0 C_{0\uparrow} + \beta_1 C_{1\uparrow} + \cdots \beta_L C_{L\uparrow}] + n_\downarrow \lambda^3 [\beta_0 C_{0\downarrow} + \beta_1 C_{1\downarrow} + \cdots \beta_L C_{L\downarrow}] = 0, \tag{A3}$$

$$\alpha_{00}(C_{0\uparrow} - C_{0\downarrow}) + \alpha_{01}(C_{1\uparrow} - C_{1\downarrow}) + \cdots + \alpha_{0L}(C_{L\uparrow} - C_{L\downarrow}) = A_0, \tag{A4}$$

$$n_\downarrow \lambda^3 [\alpha_{m0}(C_{0\uparrow} - C_{0\downarrow}) + (\alpha_{m1\uparrow} C_{1\uparrow} + \alpha_{m1\downarrow} C_{1\downarrow}) + \cdots + (\alpha_{mL\uparrow} C_{L\uparrow} + \alpha_{mL\downarrow} C_{L\downarrow})] = A_m, \tag{A5}$$

$$n_\uparrow \lambda^3 [-\alpha_{m0}(C_{0\uparrow} - C_{0\downarrow}) + (\alpha_{m1\downarrow} C_{1\uparrow} + \alpha_{m1\uparrow} C_{1\downarrow}) + \cdots + (\alpha_{mL\downarrow} C_{L\uparrow} + \alpha_{mL\uparrow} C_{L\downarrow})] = A_m. \tag{A6}$$

Here, $\{\alpha_{00},\alpha_{0n},\alpha_{m0},\alpha_{mn\sigma}\}$ ($m,n = 1,2,\ldots,L$ and $\sigma = \uparrow, \downarrow$) are dimensionless numbers which may depend on $(\lambda/a)^2$ through the exponential integral and incomplete Γ functions and implicitly depend on the order of approximation L but do not explicitly depend on temperature and densities. $\{A_\ell,\beta_\ell\}$ are determined by Gaussian integrals as follows:

$$A_\ell = \int \frac{d^3\mathbf{q}}{(2\pi)^3} \left(\frac{q^2}{4\pi} - \frac{5}{2}\right) q^{2\ell} q_z^2 e^{-q^2/4\pi} = \frac{1}{3} 2^{3+2\ell} \pi^{\frac{1}{2}+\ell} \ell \Gamma\left[\frac{5}{2} + \ell\right], \tag{A7}$$

$$\beta_\ell = \int \frac{d^3\mathbf{q}}{(2\pi)^3} q^{2\ell} q_z^2 e^{-q^2/4\pi} = \frac{1}{3} 2^{3+2\ell} \pi^{\frac{1}{2}+\ell} \Gamma\left[\frac{5}{2} + \ell\right], \tag{A8}$$

where $\Gamma[x]$ is the Γ function and A_ℓ and β_ℓ are purely numerical numbers independent of physical parameters. Note that the first equation [Eq. (A3)] fixes the frame to be $\mathbf{j}_\uparrow + \mathbf{j}_\downarrow = \mathbf{0}$. From dimensional analysis and the symmetry under $\uparrow \leftrightarrow \downarrow$, we may write an ansatz solution of the above equations in the following form ($m = 1,2,\ldots,L$):

$$C_{0\uparrow} = -\frac{1}{\lambda^3}\left(\frac{a_0}{n_\uparrow} + \frac{b_0}{n_\downarrow} + \frac{c_0}{n}\right), \tag{A9}$$

$$C_{0\downarrow} = -\frac{1}{\lambda^3}\left(\frac{b_0}{n_\uparrow} + \frac{a_0}{n_\downarrow} + \frac{c_0}{n}\right), \tag{A10}$$

$$C_{m\uparrow} = -\frac{1}{\lambda^3}\left(\frac{a_m}{n_\uparrow} + \frac{b_m}{n_\downarrow}\right), \tag{A11}$$

$$C_{m\downarrow} = -\frac{1}{\lambda^3}\left(\frac{b_m}{n_\uparrow} + \frac{a_m}{n_\downarrow}\right), \tag{A12}$$

where $\{a_\ell,b_\ell,c_0\}$ ($\ell = 0,1,2,\ldots,L$) are $2L+3$ unknown dimensionless numbers which may depend only on $(\lambda/a)^2$. Since the above set of equations should hold for any values of $n_\uparrow$ and $n_\downarrow$, once we insert the ansatz to the above equations, we obtain $2L+3$ linear equations in terms of $\{a_\ell,b_\ell,c_0\}$. Since we are still using the same set of coefficients $\{\alpha_{00},\alpha_{0n},\alpha_{m0},\alpha_{mn\sigma}\}$ and $\{\beta_\ell\}$, it is easy to see that once the original set of equations is linearly independent (which is a necessary condition to have an approximate solution of the Boltzmann equation), the set of descendent equations is also linearly independent. Therefore, once we determine all $\{a_\ell,b_\ell,c_0\}$, the above ansatz is the (Lth order) approximate solution of the Boltzmann equation.

When $\nabla p = 0$, we know that $\mathbf{j}_{\text{spin}} = -S_s' \nabla T$. It is straightforward to show that

$$S_s' = -\frac{\hbar}{m}\frac{n_\uparrow}{T}\left(\sum_{\ell=0}^{L} \beta_\ell C_{\ell\uparrow}\right) \tag{A13}$$

$$= \frac{\hbar}{m}\frac{1}{T}\frac{1}{\lambda^3}\left(\sum_{\ell=0}^{L} \beta_\ell a_\ell + \frac{n_\uparrow}{n_\downarrow}\sum_{\ell=0}^{L} \beta_\ell b_\ell + \frac{n_\uparrow}{n}\beta_0 c_0\right). \tag{A14}$$

Since $\{a_\ell,b_\ell,c_0\}$ satisfies Eq. (A3), we have two identities:

$$\sum_{\ell=0}^{L} \beta_\ell a_\ell = -\frac{1}{2}\beta_0 c_0, \tag{A15}$$

$$\sum_{\ell=0}^{L} \beta_\ell b_\ell = 0. \tag{A16}$$

Inserting these identities to Eq. (A14), we finally obtain the full polarization and temperature dependence of the Seebeck coefficient ($\beta_0 = 2\pi$).

$$S_s' = \frac{\hbar}{m}\frac{n_\uparrow - n_\downarrow}{n\lambda^3}\frac{\pi}{T} c_0. \tag{A17}$$

This proves that the scaling of Eq. (19) is indeed true at all orders of approximation. Furthermore, we see that the dimensionless scaled function $h_L(x)$ (L is the order of approximation) is

$$h_L((\lambda/a)^2) = \pi c_0. \tag{A18}$$

It should be noted that c_0 implicitly depends on the order of approximation.

For the thermal conductivity κ', we are only interested in the first term, κ_1', which directly comes from the energy current $\mathbf{j}_\epsilon$,

$$\kappa_1' = -\frac{1}{4\pi}\frac{\hbar}{m}\sum_{\ell=0}^{L} B_\ell (n_\uparrow C_{\ell\uparrow} + n_\downarrow C_{\ell\downarrow}), \tag{A19}$$

where $B_\ell = 4\pi(5/2+\ell)\beta_\ell$. Plugging in ansatz solution and using Eq. (A3), we obtain κ_1',

$$\kappa_1' = \frac{\hbar}{m}\frac{1}{\lambda^3}\sum_{\ell=1}^{L}\left(\frac{n_\uparrow^2 b_\ell + 2n_\uparrow n_\downarrow a_\ell + n_\downarrow^2 b_\ell}{n_\uparrow n_\downarrow}\right)\ell\beta_\ell. \tag{A20}$$

Again, we emphasize that a_ℓ and b_ℓ are function of $(\lambda/a)^2$ and implicitly depend on the order of approximation. This proves that the algebraic form of the polarization dependence of the thermal conductivity obtained in the main text remains to all orders of approximation.

2. D_s and P_s'

Now we study D_s and P_s' when $\nabla T = 0$ (thus, $\nabla n = 0$). As we did in the previous subsection, we want to express $\nabla n_\uparrow$ and $\nabla n_\downarrow$ in terms of $n\nabla p$.

$$\frac{\nabla n_i}{n_i} = \epsilon^i \frac{n\nabla p}{2n_i}, \tag{A21}$$

where $\epsilon^{\uparrow}=1$ and $\epsilon^{\downarrow}=-1$. Then, the ansatz [Eq. (13)] takes the following form ($i\neq j$):

$$\psi_i=-\epsilon^i\lambda\frac{n}{2}\sum_{\ell=0}^{L}\left(\frac{C_{\ell ii}}{n_i}-\frac{C_{\ell ij}}{n_j}\right)q_i^{2\ell}\mathbf{q}_i\cdot\nabla p. \quad \text{(A22)}$$

Once we define

$$\tilde{C}_{\ell i}\equiv-\frac{n}{2}\left(\frac{C_{\ell ii}}{n_i}-\frac{C_{\ell ij}}{n_j}\right), \quad \text{(A23)}$$

we reduce the system similar to the previous case. The $2(L+1)$ linearly independent equations are ($m=1,2,\ldots L$)

$$n_{\uparrow}\lambda^3[\beta_0\tilde{C}_{0\uparrow}+\beta_1\tilde{C}_{1\uparrow}+\cdots\beta_L\tilde{C}_{L\uparrow}] -n_{\downarrow}\lambda^3[\beta_0\tilde{C}_{0\downarrow}+\beta_1\tilde{C}_{1\downarrow}+\cdots\beta_L\tilde{C}_{L\downarrow}]=0, \quad \text{(A24)}$$

$$\alpha_{00}(\tilde{C}_{0\uparrow}+\tilde{C}_{0\downarrow})+\alpha_{01}(\tilde{C}_{1\uparrow}+\tilde{C}_{1\downarrow}) +\cdots+\alpha_{0L}(\tilde{C}_{L\uparrow}+\tilde{C}_{L\downarrow})=\tilde{A}_0, \quad \text{(A25)}$$

$$\frac{n_{\uparrow}n_{\downarrow}\lambda^3}{n}[\alpha_{m0}(\tilde{C}_{0\uparrow}+\tilde{C}_{0\downarrow})+(\alpha_{m1\uparrow}\tilde{C}_{1\uparrow}-\alpha_{m1\downarrow}\tilde{C}_{1\downarrow}) +\cdots+(\alpha_{mL\uparrow}\tilde{C}_{L\uparrow}-\alpha_{mL\downarrow}\tilde{C}_{L\downarrow})]=\tilde{A}_m, \quad \text{(A26)}$$

$$\frac{n_{\uparrow}n_{\downarrow}\lambda^3}{n}[-\alpha_{m0}(\tilde{C}_{0\uparrow}+\tilde{C}_{0\downarrow})+(\alpha_{m1\downarrow}\tilde{C}_{1\uparrow}-\alpha_{m1\uparrow}\tilde{C}_{1\downarrow}) +\cdots+(\alpha_{mL\downarrow}\tilde{C}_{L\uparrow}-\alpha_{mL\uparrow}\tilde{C}_{L\downarrow})]=-\tilde{A}_m. \quad \text{(A27)}$$

$\alpha's$ and β_ℓ are same as in the previous section and $\tilde{A}_\ell=\beta_\ell$.

Although coefficients of Eqs. (A26) and (A27) are linearly dependent, once we combine them, we obtain another L linearly independent equation,

$$\sum_{n=1}^{L}(\alpha_{mn\uparrow}-\alpha_{mn\downarrow})(\tilde{C}_{n\uparrow}-\tilde{C}_{n\downarrow})=0. \quad \text{(A28)}$$

Together with Eq. (A28), we have $2(L+1)$ linearly independent equations that uniquely determine all $\tilde{C}_{\ell i}$.

First observe that the solution of Eq. (A28) is trivial; $\tilde{C}_{m\uparrow}=\tilde{C}_{m\downarrow}$. Then, we use the following ansatz [39]:

$$\tilde{C}_{0\uparrow}=-\frac{1}{\lambda^3}\left(\frac{\tilde{a}_0}{n_{\uparrow}}+\frac{\tilde{b}_0}{n_{\downarrow}}\right), \quad \text{(A29)}$$

$$\tilde{C}_{0\uparrow}=-\frac{1}{\lambda^3}\left(\frac{\tilde{b}_0}{n_{\uparrow}}+\frac{\tilde{a}_0}{n_{\downarrow}}\right), \quad \text{(A30)}$$

$$\tilde{C}_{m\uparrow}=-\frac{1}{\lambda^3}\frac{n\tilde{c}_m}{n_{\uparrow}n_{\downarrow}}=\tilde{C}_{m\downarrow}. \quad \text{(A31)}$$

$\{\tilde{a}_0,\tilde{b}_0,\tilde{c}_m\}$ are dimensionless numbers that may only depend on $(\lambda/a)^2$. Substituting the above into original linear equations, we obtain the same linearly independent equations in terms of $\{\tilde{a}_0,\tilde{b}_0,\tilde{c}_m\}$. Therefore, once we determine them, we have the approximate solution of the Boltzmann equation.

Following the same procedure when we obtained S_s' and κ_1', we can show that

$$D_s=\frac{\hbar}{m}\frac{2\pi}{\lambda^3}(\tilde{a}_0-\tilde{b}_0), \quad \text{(A32)}$$

$$P_{s1}'=\frac{\hbar}{m}\frac{T}{n\lambda^3}\sum_{\ell=1}^{L}\left(\frac{n_{\uparrow}^2-n_{\downarrow}^2}{n_{\uparrow}n_{\downarrow}}\right)\tilde{c}_\ell\ell\beta_\ell, \quad \text{(A33)}$$

where P_{s1}' is the first term in the Peltier coefficient. Once we scale the scattering length with λ, the polarization and temperature dependence of D_s and P_{s1}' at an arbitrary L remains the same as for $L=1$. This proves that the scaling structure of the transport coefficients remains the same to all orders of approximation.

APPENDIX B: CALCULATION OF THE SPIN SEEBECK EFFECT

Here we present derivations of signatures of the spin Seebeck effect in detail. First, apply a long-wavelength temperature modulation to the system. The mechanical equilibrium condition implies that a temperature modulation is equivalent to a total density modulation. Initially the gas is uniformly polarized so that the density of each spin component is

$$n_i(t=0,z)=n_{i0}+\delta n_{i0}\cos wz, \quad \text{(B1)}$$

$$\delta n_{i0}=\frac{n_{i0}}{n_0}\delta n_0, \quad \text{(B2)}$$

where δn_0 is the maximum value of total density deviation from the average density. In order to calculate the change of densities of each species, which is directly measurable in experiment and contains the signature of the spin Seebeck effect, we need the space-time dependence of the density of each species. We use the diffusion matrix and the continuity equation to derive the space-time dependence of densities. Since the continuity equation for the particle number density is $\partial_t n_i+\nabla\cdot\mathbf{j}_i=0$, it is practical to write diffusion equation in the format of Eq. (1). With this initial condition, a nonuniform particle current flows, but in this classical limit, there is no net energy current. Thus, we work in the reference frame where the local energy current vanishes ($\mathbf{j}_{\epsilon\uparrow}+\mathbf{j}_{\epsilon\downarrow}=0$). Thanks to Galilean invariance, this choice of a reference frame does not affect the physics.

Following a similar procedure as described in the main text, but in this zero energy current frame, we can determine all coefficients $C_{\ell ij}$ ($\ell=0,1$) and express the particle current of each species in terms of $\nabla n_{\uparrow}$ and $\nabla n_{\downarrow}$. Then, we can write currents in the diffusion matrix format as in Eq. (1). Near unitarity,

$$\begin{pmatrix}\mathbf{j}_{\uparrow}\\ \mathbf{j}_{\downarrow}\end{pmatrix}=-\frac{9\pi^{3/2}}{9728\sqrt{2}}\left(\frac{\hbar}{m}\left(\frac{T}{T_F}\right)^{3/2}\right) \times\begin{pmatrix}\frac{365n_{\uparrow}^2+354n_{\uparrow}n_{\downarrow}+733n_{\downarrow}^2}{nn_{\downarrow}} & \frac{381n_{\uparrow}^2+42n_{\uparrow}n_{\downarrow}+405n_{\downarrow}^2}{nn_{\downarrow}}\\ \frac{405n_{\uparrow}^2+42n_{\uparrow}n_{\downarrow}+381n_{\downarrow}^2}{nn_{\uparrow}} & \frac{733n_{\uparrow}^2+354n_{\uparrow}n_{\downarrow}+365n_{\downarrow}^2}{nn_{\uparrow}}\end{pmatrix} \times\begin{pmatrix}\nabla n_{\uparrow}\\ \nabla n_{\downarrow}\end{pmatrix}. \quad \text{(B3)}$$

Far from unitarity,

$$\begin{pmatrix}\mathbf{j}_\uparrow\\ \mathbf{j}_\downarrow\end{pmatrix} = -\frac{3\pi^{3/2}}{896\sqrt{2}}\left(\frac{\hbar}{m(k_Fa)^2}\sqrt{\frac{T}{T_F}}\right) \times\begin{pmatrix}\frac{145n_\uparrow^2+158n_\uparrow n_\downarrow+289n_\downarrow^2}{nn_\downarrow} & \frac{137n_\uparrow^2-14n_\uparrow n_\downarrow+125n_\downarrow^2}{nn_\downarrow}\\ \frac{125n_\uparrow^2-14n_\uparrow n_\downarrow+137n_\downarrow^2}{nn_\uparrow} & \frac{289n_\uparrow^2+158n_\uparrow n_\downarrow+145n_\downarrow^2}{nn_\uparrow}\end{pmatrix} \times\begin{pmatrix}\nabla n_\uparrow\\ \nabla n_\downarrow\end{pmatrix}. \tag{B4}$$

These matrix equations contain two eigenmodes: One is the thermal mode with eigenvalue $\mathfrak{D}_T$ ($\mathbf{j}_\uparrow$ and $\mathbf{j}_\downarrow$ are in the same directions) and the other is the spin mode with eigenvalue $\mathfrak{D}_s$ ($\mathbf{j}_\uparrow$ and $\mathbf{j}_\downarrow$ are in opposite directions). As expected, $\mathfrak{D}_T > \mathfrak{D}_s$ for all polarizations in both of these limits. Applying continuity equations to the above diffusion matrix equations while keeping all differential operators linear (we restrict ourselves in a linear response theory), we obtain two-component diffusion equations:

$$\frac{\partial}{\partial t}\begin{pmatrix}n_\uparrow\\ n_\downarrow\end{pmatrix} = -\begin{pmatrix}\mathfrak{D}_{\uparrow\uparrow} & \mathfrak{D}_{\uparrow\downarrow}\\ \mathfrak{D}_{\downarrow\uparrow} & \mathfrak{D}_{\downarrow\downarrow}\end{pmatrix}\begin{pmatrix}\nabla^2 n_\uparrow\\ \nabla^2 n_\downarrow\end{pmatrix}. \tag{B5}$$

Therefore, we can immediately write the time evolution of each species in terms of the eigenmodes as

$$\begin{pmatrix}n_\uparrow(t,z)\\ n_\downarrow(t,z)\end{pmatrix} = \begin{pmatrix}n_{\uparrow0}\\ n_{\downarrow0}\end{pmatrix} + \alpha e^{-\mathfrak{D}_s w^2 t}\delta n_{\downarrow0}\begin{pmatrix}\gamma\\ 1\end{pmatrix}\cos wz + \beta e^{-\mathfrak{D}_T w^2 t}\delta n_{\downarrow0}\begin{pmatrix}\zeta\\ 1\end{pmatrix}\cos wz. \tag{B6}$$

$(\gamma, 1)$ and $(\zeta, 1)$ are the eigenvectors of the spin mode and the thermal mode, respectively. γ is negative while ζ is positive. α and β are determined by the initial condition,

$$\begin{pmatrix}\delta n_{\uparrow0}\\ \delta n_{\downarrow0}\end{pmatrix} = \alpha\delta n_{\downarrow0}\begin{pmatrix}\gamma\\ 1\end{pmatrix} + \beta\delta n_{\downarrow0}\begin{pmatrix}\zeta\\ 1\end{pmatrix}. \tag{B7}$$

It is straightforward to derive γ, ζ, α, β, $\mathfrak{D}_s$, and $\mathfrak{D}_T$. For example,

$$\alpha = \frac{1}{\gamma-\zeta}\left(\frac{n_{0\uparrow}}{n_{0\downarrow}} - \zeta\right), \tag{B8}$$

$$\beta = 1-\alpha. \tag{B9}$$

Explicit expressions for γ, ζ, $\mathfrak{D}_s$, and $\mathfrak{D}_T$ are fairly lengthy so they are omitted here.

The spin Seebeck effect is most apparent when observing the densities at the edges of the system ($wz = 0$ or $wz = \pi$) so we choose to focus on the cold edge, $z = 0$. The uniform pressure condition implies that both majority and minority densities are initially higher than average at the cold side. Thus, initially $\delta n_\downarrow(t = 0, z = 0) > 0$. Even though the initial condition can be chosen to be the same for both unitarity and far away from unitarity, the time evolution of density of each species is qualitatively different for these two limiting cases. As argued in the main text, the minority density deviation has an extremum before it relaxes to zero at unitarity, whereas the majority density deviation has an extremum far away from unitarity. Therefore, a change in the sign of a certain species is a unique signature of the spin Seebeck effect. We can express the magnitude of the spin Seebeck signal in dimensionless form by $\frac{\delta n_i(t,0)}{\delta n_{i0}}$. This quantity is plotted in Figs. 3 and 4. At time $t_{i,\mathrm{ext}}$ ($i = \downarrow$ near unitarity and $i = \uparrow$ away from unitarity), the density of the species i reaches an extremum. It is easy to derive formal expressions of $t_{i,\mathrm{ext}}$ and a dimensionless measure, $|\frac{\delta n_i(t_{i,\mathrm{ext}},0)}{\delta n_{i0}}|$.

Near unitarity,

$$t_{\downarrow,\mathrm{ext}} = \frac{1}{(\mathfrak{D}_T-\mathfrak{D}_s)w^2}\ln\left|\frac{\mathfrak{D}_T\beta}{\mathfrak{D}_s\alpha}\right|, \tag{B10}$$

$$\left|\frac{\delta n_\downarrow(t_{\downarrow,\mathrm{ext}},0)}{\delta n_{\downarrow0}}\right| = \alpha\exp\left[-\frac{\mathfrak{D}_s}{\mathfrak{D}_T-\mathfrak{D}_s}\ln\left|\frac{\mathfrak{D}_T\beta}{\mathfrak{D}_s\alpha}\right|\right] + \beta\exp\left[-\frac{\mathfrak{D}_T}{\mathfrak{D}_T-\mathfrak{D}_s}\ln\left|\frac{\mathfrak{D}_T\beta}{\mathfrak{D}_s\alpha}\right|\right]. \tag{B11}$$

Away from unitarity,

$$t_{\uparrow,\mathrm{ext}} = \frac{1}{(\mathfrak{D}_T-\mathfrak{D}_s)w^2}\ln\left|\frac{\mathfrak{D}_T\beta\zeta}{\mathfrak{D}_s\alpha\gamma}\right|, \tag{B12}$$

$$\left|\frac{\delta n_\uparrow(t_{\uparrow,\mathrm{ext}},0)}{\delta n_{\uparrow0}}\right| = \frac{\alpha\gamma}{\alpha\gamma+\beta\zeta}\exp\left[-\frac{\mathfrak{D}_s}{\mathfrak{D}_T-\mathfrak{D}_s}\ln\left|\frac{\mathfrak{D}_T\beta\zeta}{\mathfrak{D}_s\alpha\gamma}\right|\right] + \frac{\beta\zeta}{\alpha\gamma+\beta\zeta}\exp\left[-\frac{\mathfrak{D}_T}{\mathfrak{D}_T-\mathfrak{D}_s}\ln\left|\frac{\mathfrak{D}_T\beta\zeta}{\mathfrak{D}_s\alpha\gamma}\right|\right]. \tag{B13}$$

$|\frac{\delta n_i(t_{i,\mathrm{ext}},0)}{\delta n_{i0}}|$ is plotted in Fig. 6. As expected, the unitarity limit shows a stronger signal of the spin Seebeck effect than far away from unitarity.

Another consequence of the spin Seebeck effect is the change of polarization. From Eqs. (B2) and (B6), we can express the polarization as a function of time. Keeping only the linear term of δn_0, we obtain

$$\delta p(t,0) = p(t,0) - p_0 = \frac{\delta n_0}{n_0}\left[\frac{n_{\downarrow0}}{n_0}\left(\alpha(\gamma-1)e^{-\mathfrak{D}_s w^2 t} + \beta(\zeta-1)e^{-\mathfrak{D}_T w^2 t}\right) - p_0\frac{n_{\downarrow0}}{n_0}\left(\alpha(\gamma+1)e^{-\mathfrak{D}_s w^2 t} + \beta(\zeta+1)e^{-\mathfrak{D}_T w^2 t}\right)\right], \tag{B14}$$

where $p_0 = (n_{\uparrow0} - n_{\downarrow0})/n_0$. Figure 5 is the plot of $\delta p(t,0)$ normalized by $\delta n_0/n_0$.

APPENDIX C: MANIFESTATION OF THE ONSAGER RELATION

For completeness, we present diffusion matrices of approximate solutions and the solution of the first-order perturbation of the Maxwellian model in the form of Eq. (2) where the Onsager relation should be explicit. We simply transform the set of driving forces $(\nabla T, n\nabla p)$ to another set of driving forces $[\nabla T, \nabla(\mu_\uparrow - \mu_\downarrow)]$ associated with the entropy production.

For approximate solutions we have the following.

At unitarity ($|a| \gg \lambda$),

$$\begin{pmatrix} \mathbf{j}_{\text{heat}} \\ \mathbf{j}_{\text{spin}} \end{pmatrix} = -\frac{45\pi^{3/2}}{608\sqrt{2}} \left(\frac{\hbar}{m}\left(\frac{T}{T_F}\right)^{3/2}\right) \begin{pmatrix} \kappa_u & (n_\uparrow - n_\downarrow) - \frac{39n_\uparrow n_\downarrow}{5n} \ln\left(\frac{n_\uparrow}{n_\downarrow}\right) \\ \frac{(n_\uparrow - n_\downarrow)}{T} - \frac{39n_\uparrow n_\downarrow}{5nT} \ln\left(\frac{n_\uparrow}{n_\downarrow}\right) & \frac{39n_\uparrow n_\downarrow}{5nT} \end{pmatrix} \begin{pmatrix} \nabla T \\ \nabla(\mu_\uparrow - \mu_\downarrow) \end{pmatrix}, \tag{C1}$$

where κ_u is

$$\kappa_u = \frac{5}{16} n \left(\frac{(73n_\uparrow^2 + 82n_\uparrow n_\downarrow + 73n_\downarrow^2)}{n_\uparrow n_\downarrow}\right) - \ln\left(\frac{n_\uparrow}{n_\downarrow}\right)\left(\frac{10(n_\uparrow^2 - n_\downarrow^2) - 39n_\uparrow n_\downarrow \ln(n_\uparrow/n_\downarrow)}{5n}\right). \tag{C2}$$

Far away from unitarity ($|a| \ll \lambda$),

$$\begin{pmatrix} \mathbf{j}_{\text{heat}} \\ \mathbf{j}_{\text{spin}} \end{pmatrix} = -\frac{15\pi^{3/2}}{224\sqrt{2}} \left(\frac{\hbar}{m(k_F a)^2}\sqrt{\frac{T}{T_F}}\right) \begin{pmatrix} \kappa_a & -(n_\uparrow - n_\downarrow) - \frac{43n_\uparrow n_\downarrow}{5n} \ln\left(\frac{n_\uparrow}{n_\downarrow}\right) \\ -\frac{(n_\uparrow - n_\downarrow)}{T} - \frac{43n_\uparrow n_\downarrow}{5nT} \ln\left(\frac{n_\uparrow}{n_\downarrow}\right) & \frac{43n_\uparrow n_\downarrow}{5nT} \end{pmatrix} \begin{pmatrix} \nabla T \\ \nabla(\mu_\uparrow - \mu_\downarrow) \end{pmatrix}, \tag{C3}$$

where κ_a is

$$\kappa_a = \frac{5}{8} n \left(\frac{(29n_\uparrow^2 + 26n_\uparrow n_\downarrow + 29n_\downarrow^2)}{n_\uparrow n_\downarrow}\right) + \ln\left(\frac{n_\uparrow}{n_\downarrow}\right)\left(\frac{10(n_\uparrow^2 - n_\downarrow^2) + 43n_\uparrow n_\downarrow \ln(n_\uparrow/n_\downarrow)}{5n}\right). \tag{C4}$$

For the first order perturbation of the Maxwellian model, we have the following:

$$\begin{pmatrix} \mathbf{j}_{\text{heat}} \\ \mathbf{j}_{\text{spin}} \end{pmatrix} = -D_0 \begin{pmatrix} \kappa_M & -\frac{\pi\epsilon(n_\uparrow - n_\downarrow)}{\lambda^2} - \frac{n_\uparrow n_\downarrow}{5n}\left(1 - \frac{20\pi\epsilon}{\lambda^2}\right) \ln\left(\frac{n_\uparrow}{n_\downarrow}\right) \\ -\frac{\pi\epsilon(n_\uparrow - n_\downarrow)}{\lambda^2 T} - \frac{n_\uparrow n_\downarrow}{5nT}\left(1 - \frac{20\pi\epsilon}{\lambda^2}\right) \ln\left(\frac{n_\uparrow}{n_\downarrow}\right) & \frac{n_\uparrow n_\downarrow}{5nT}\left(1 - \frac{20\pi\epsilon}{\lambda^2}\right) \end{pmatrix} \begin{pmatrix} \nabla T \\ \nabla(\mu_\uparrow - \mu_\downarrow) \end{pmatrix}, \tag{C5}$$

where κ_M is

$$\kappa_M = \frac{1}{2} n \left(\frac{(n_\uparrow^2 + n_\uparrow n_\downarrow + n_\downarrow^2)}{n_\uparrow n_\downarrow} - \frac{3\pi\epsilon}{\lambda^2}\frac{(9n_\uparrow^2 + 10n_\uparrow n_\downarrow + 9n_\downarrow^2)}{n_\uparrow n_\downarrow}\right) + \frac{2\pi\epsilon \ln\left(\frac{n_\uparrow}{n_\downarrow}\right)}{n\lambda^2}\left((n_\uparrow^2 - n_\downarrow^2) + n_\uparrow n_\downarrow\left(\frac{\lambda^2}{10\pi\epsilon} - 2\right)\ln\left(\frac{n_\uparrow}{n_\downarrow}\right)\right) \tag{C6}$$

The above matrices clearly exhibit the Onsager relation. Also each off-diagonal element carries a term proportional to $-\sigma_s \ln(n_\uparrow/n_\downarrow)$ as mentioned in Eq. (32) in Sec. VI. Last, the structure of thermal conductivity [Eq. (38)] is evident.

[1] A. Sommer, M. Ku, G. Roati, and M. W. Zwierlein, Nature (London) **472**, 201 (2011).

[2] A. Sommer, M. Ku, and M. W. Zwierlein, New J. Phys. **13**, 055009 (2011).

[3] N. Strohmaier, Y. Takasu, K. Günter, R. Jördens, M. Köhl, H. Moritz, and T. Esslinger, Phys. Rev. Lett. **99**, 220601 (2007).

[4] M. Pasienski, D. McKay, M. White, and B. DeMarco, Nat. Phys. **6**, 677 (2010).

[5] A. Trenkwalder, C. Kohstall, M. Zaccanti, D. Naik, A. I. Sidorov, F. Schreck, and R. Grimm, Phys. Rev. Lett. **106**, 115304 (2011).

[6] Y. A. Liao, M. Revelle, T. Paprotta, A. S. C. Rittner, W. Li, G. B. Partridge, and R. G. Hulet, Phys. Rev. Lett. **107**, 145305 (2011).

[7] M. J. H. Ku, A. T. Sommer, L. W. Cheuk, and M. W. Zwierlein, Science **335**, 563 (2012).

[8] S. Nascimbene, N. Navon, K. J. Jiang, F. Chevy, and C. Salomon, Nature (London) **463**, 1057 (2010).

[9] H. Smith and H. H. Jensen, *Transport Phenomena* (Clarendon Press, Oxford, 1989), Chap. 1.

[10] S. A. Wolf, D. D. Awschalom, R. A. Buhrman, J. M. Daughton, S. von Molnar, M. L. Roukes, A. Y. Chtchelkanova, and D. M. Treger, Science **294**, 1488 (2001).

[11] T. Kimura, Y. Otani, T. Sato, S. Takahashi, and S. Maekawa, Phys. Rev. Lett. **98**, 156601 (2007).

[12] K. Uchida, S. Takahashi, K. Harii, J. Ieda, W. Koshibae, K. Ando, S. Maekawa, and E. Saitoh, Nature (London) **455**, 778 (2008).

[13] J. Flipse, F. L. Bakker, A. Slachter, F. K. Dejene, and B. J. van Wees, Nat. Nanotechnol. **7**, 166 (2012).

[14] C. H. Wong, H. T. C. Stoof, and R. A. Duine, Phys. Rev. A **85**, 063613 (2012).

[15] C. Grenier, C. Kollath, and A. Georges, arXiv:1209.3942v2.

[16] W. Ketterle and M. W. Zwierlein, arXiv:0801.2500v1.

[17] N. Navon, S. Nascimbene, F. Chevy, and C. Salomon, Science **328**, 729 (2010).

[18] C. A. Regal and D. S. Jin, Phys. Rev. Lett. **90**, 230404 (2003).

[19] K. M. O'Hara, S. L. Hemmer, S. R. Granade, M. E. Gehm, J. E. Thomas, V. Venturi, E. Tiesinga, and C. J. Williams, Phys. Rev. A **66**, 041401 (2002).

[20] P. M. Chaikin and T. C. Lubensky, *Principles of Condensed Matter Physics* (Cambridge University Press, Cambridge, 1995), Chap. 8.

[21] G. M. Bruun, New J. Phys. **13**, 035005 (2011).
[22] G. M. Bruun, A. Recati, C. J. Pethick, H. Smith, and S. Stringari, Phys. Rev. Lett. **100**, 240406 (2008).
[23] H. Kim and D. A. Huse, Phys. Rev. A **85**, 043603 (2012).
[24] A. Bulgac, M. McNeil Forbes, and A. Schwenk, Phys. Rev. Lett. **97**, 020402 (2006).
[25] D. E. Sheehy and L. Radzihovsky, Ann. Phys. **322**, 1790 (2007).
[26] A. Bulgac and M. McNeil Forbes, Phys. Rev. Lett. **101**, 215301 (2008).
[27] Y. Liao, A. S. C. Rittner, T. Paprotta, W. Li, G. B. Partridge, R. G. Hulet, S. K. Baur, and E. J. Mueller, Nature (London) **467**, 567 (2010).
[28] G. M. Bruun, A. D. Jackson, and E. E. Kolomeitsev, Phys. Rev. A **71**, 052713 (2005).
[29] S. Chiacchiera, T. Lepers, D. Davesne, and M. Urban, Phys. Rev. A **79**, 033613 (2009).
[30] A. M. Clogston, Phys. Rev. Lett. **9**, 266 (1962).
[31] B. S. Chandrasekhar, Appl. Phys. Lett. **1**, 7 (1962).
[32] M. W. Zwierlein, A. Schirotzek, C. H. Schunck, and W. Ketterle, Science **311**, 492 (2006).
[33] Y. Shin, M. W. Zwierlein, C. H. Schunck, A. Schirotzek, and W. Ketterle, Phys. Rev. Lett. **97**, 030401 (2006).
[34] In the limit of high temperature, a gas is still dilute enough so that kinetic energy gives the dominant contribution to the total energy. This is a necessary condition to use the Boltzmann approach.
[35] S. Chiacchiera, T. Lepers, D. Davesne, and M. Urban, Phys. Rev. A **84**, 043634 (2011).
[36] H. Mori, Phys. Rev. **112**, 1829 (1958).
[37] J. M. Luttinger, Phys. Rev. **135**, A1505 (1964).
[38] Since $5T/2$ is the thermal average enthalpy per particle in classical regime, $\tilde{\mathbf{j}}_{\text{heat}}$ is the local energy current relative to the local average motion of the gas.
[39] Motivation of this choice came from the observation that the right-hand side of the linear equation does not depend on densities. Therefore, a quantity in the big parentheses in the left-hand side must be proportional to $n/(n_\uparrow n_\downarrow)$.